

AD-A221 560

REPORT DOCUMENTATION PAGE			Form Approved OMB No. 0704-0188	
DTIC TITLE COPY				
1. AGENCY USE ONLY (Leave blank)		2. REPORT DATE	3. REPORT TYPE AND DATES COVERED	
			FINAL 15 Jul 89 TO 14 Jan 90	
4. TITLE AND SUBTITLE			5. FUNDING NUMBERS	
Fabrication of Microwave Guides using High T <sub>c</sub> Superconductors			D822/F1 SDI	
6. AUTHOR(S)			APR 30 1990	
Dr Sudhir B. Trivedi			D	
7. PERFORMING ORGANIZATION NAME(S) AND ADDRESS(ES)			8. PERFORMING ORGANIZATION REPORT NUMBER	
Brimrose Corporation of America 5020 Campbell Blvd Baltimore, MD 21236			APOSR-TK-90-051	
9. SPONSORING MONITORING AGENCY NAME(S) AND ADDRESS(ES)			10. SPONSORING MONITORING AGENCY REPORT NUMBER	
AFOSR/NE Bldg 410 Bolling AFB Washington DC 20332-6448 Dr. Harold Weinstock			F49620-89-C-0111	
11. SUPPLEMENTARY NOTES			REPRODUCED BY U.S. DEPARTMENT OF COMMERCE NATIONAL TECHNICAL INFORMATION SERVICE SPRINGFIELD VA 22161	
12a. DISTRIBUTION AVAILABILITY STATEMENT			12b. DISTRIBUTION CODE	
APPROVED FOR PUBLIC RELEASE: DISTRIBUTION IS UNLIMITED				
13. ABSTRACT (Maximum 200 words)				
The present study indicates that optimization of microstructure can improve the microwave conductivity of YBa <sub>2</sub> Cu <sub>3</sub> O <sub>7-x</sub> . Optimum microstructure here refers to large grain size and better grain-to-grain contact. (2) In the present study we determined that YBa <sub>2</sub> Cu <sub>3</sub> O <sub>7-x</sub> processed (oxygen annealed) at 960°C and 975°C yield grain size in the range of 60um - 150um. (3) Addition of the optimum amount of gold to YBa <sub>2</sub> Cu <sub>3</sub> O <sub>7-x</sub> results in a sharp superconducting transition and zero resistivity temperatures. (4) Addition of gold also improves the microwave conductivity of YBa <sub>2</sub> Cu <sub>3</sub> O <sub>7-x</sub> . (5) YBa <sub>2</sub> Cu <sub>3</sub> O <sub>7-x</sub> processed at 960°C has conductivity equal to about 90% the conductivity of copper at 16 GHz. Addition of 10% of gold to this material increases its conductivity to about 97% of the conductivity of copper at about 16 GHz. Addition of 20% of gold to this material deteriorates its microwave conductivity. (6) Interpolation of the results on microwave conductivity at 16 GHz to lower frequencies suggests that at lower frequencies our material has microwave conductivity higher than that of copper.				
14. SUBJECT TERMS			15. NUMBER OF PAGES	
			16. PRICE CODE	
17. SECURITY CLASSIFICATION OF REPORT	18. SECURITY CLASSIFICATION OF THIS PAGE	19. SECURITY CLASSIFICATION OF ABSTRACT	20. LIMITATION OF ABSTRACT	
UNCLASSIFIED	UNCLASSIFIED	UNCLASSIFIED	UNLIMITED	



APOSR-TR-90-0510

brimrose corporation of america • 5020 campbell blvd. • baltimore, maryland 21236  
301/529-5800 • fax: 301/529-9491

FABRICATION OF MICROWAVE WAVE GUIDES  
USING  
HIGH  $T_c$  SUPERCONDUCTORS

AMT  
APR 1990

FINAL REPORT

Sponsored by

USAF, AFSC  
Air Force Office of Scientific Research  
Bolling AFB, DC 20332-6448

Contract #F49620-89-C-0111

1  
2  
3  
4  
5  
6  
7  
8  
9  
10  
11  
12  
13  
14  
15  
16  
17  
18  
19  
20  
21  
22  
23  
24  
25  
26  
27  
28  
29  
30  
31  
32  
33  
34  
35  
36  
37  
38  
39  
40  
41  
42  
43  
44  
45  
46  
47  
48  
49  
50  
51  
52  
53  
54  
55  
56  
57  
58  
59  
60  
61  
62  
63  
64  
65  
66  
67  
68  
69  
70  
71  
72  
73  
74  
75  
76  
77  
78  
79  
80  
81  
82  
83  
84  
85  
86  
87  
88  
89  
90  
91  
92  
93  
94  
95  
96  
97  
98  
99  
100  
101  
102  
103  
104  
105  
106  
107  
108  
109  
110  
111  
112  
113  
114  
115  
116  
117  
118  
119  
120  
121  
122  
123  
124  
125  
126  
127  
128  
129  
130  
131  
132  
133  
134  
135  
136  
137  
138  
139  
140  
141  
142  
143  
144  
145  
146  
147  
148  
149  
150  
151  
152  
153  
154  
155  
156  
157  
158  
159  
160  
161  
162  
163  
164  
165  
166  
167  
168  
169  
170  
171  
172  
173  
174  
175  
176  
177  
178  
179  
180  
181  
182  
183  
184  
185  
186  
187  
188  
189  
190  
191  
192  
193  
194  
195  
196  
197  
198  
199  
200  
201  
202  
203  
204  
205  
206  
207  
208  
209  
210  
211  
212  
213  
214  
215  
216  
217  
218  
219  
220  
221  
222  
223  
224  
225  
226  
227  
228  
229  
230  
231  
232  
233  
234  
235  
236  
237  
238  
239  
240  
241  
242  
243  
244  
245  
246  
247  
248  
249  
250  
251  
252  
253  
254  
255  
256  
257  
258  
259  
260  
261  
262  
263  
264  
265  
266  
267  
268  
269  
270  
271  
272  
273  
274  
275  
276  
277  
278  
279  
280  
281  
282  
283  
284  
285  
286  
287  
288  
289  
290  
291  
292  
293  
294  
295  
296  
297  
298  
299  
300  
301  
302  
303  
304  
305  
306  
307  
308  
309  
310  
311  
312  
313  
314  
315  
316  
317  
318  
319  
320  
321  
322  
323  
324  
325  
326  
327  
328  
329  
330  
331  
332  
333  
334  
335  
336  
337  
338  
339  
340  
341  
342  
343  
344  
345  
346  
347  
348  
349  
350  
351  
352  
353  
354  
355  
356  
357  
358  
359  
360  
361  
362  
363  
364  
365  
366  
367  
368  
369  
370  
371  
372  
373  
374  
375  
376  
377  
378  
379  
380  
381  
382  
383  
384  
385  
386  
387  
388  
389  
390  
391  
392  
393  
394  
395  
396  
397  
398  
399  
400  
401  
402  
403  
404  
405  
406  
407  
408  
409  
410  
411  
412  
413  
414  
415  
416  
417  
418  
419  
420  
421  
422  
423  
424  
425  
426  
427  
428  
429  
430  
431  
432  
433  
434  
435  
436  
437  
438  
439  
440  
441  
442  
443  
444  
445  
446  
447  
448  
449  
450  
451  
452  
453  
454  
455  
456  
457  
458  
459  
460  
461  
462  
463  
464  
465  
466  
467  
468  
469  
470  
471  
472  
473  
474  
475  
476  
477  
478  
479  
480  
481  
482  
483  
484  
485  
486  
487  
488  
489  
490  
491  
492  
493  
494  
495  
496  
497  
498  
499  
500  
501  
502  
503  
504  
505  
506  
507  
508  
509  
510  
511  
512  
513  
514  
515  
516  
517  
518  
519  
520  
521  
522  
523  
524  
525  
526  
527  
528  
529  
530  
531  
532  
533  
534  
535  
536  
537  
538  
539  
540  
541  
542  
543  
544  
545  
546  
547  
548  
549  
550  
551  
552  
553  
554  
555  
556  
557  
558  
559  
560  
561  
562  
563  
564  
565  
566  
567  
568  
569  
570  
571  
572  
573  
574  
575  
576  
577  
578  
579  
580  
581  
582  
583  
584  
585  
586  
587  
588  
589  
590  
591  
592  
593  
594  
595  
596  
597  
598  
599  
600  
601  
602  
603  
604  
605  
606  
607  
608  
609  
610  
611  
612  
613  
614  
615  
616  
617  
618  
619  
620  
621  
622  
623  
624  
625  
626  
627  
628  
629  
630  
631  
632  
633  
634  
635  
636  
637  
638  
639  
640  
641  
642  
643  
644  
645  
646  
647  
648  
649  
650  
651  
652  
653  
654  
655  
656  
657  
658  
659  
660  
661  
662  
663  
664  
665  
666  
667  
668  
669  
670  
671  
672  
673  
674  
675  
676  
677  
678  
679  
680  
681  
682  
683  
684  
685  
686  
687  
688  
689  
690  
691  
692  
693  
694  
695  
696  
697  
698  
699  
700  
701  
702  
703  
704  
705  
706  
707  
708  
709  
710  
711  
712  
713  
714  
715  
716  
717  
718  
719  
720  
721  
722  
723  
724  
725  
726  
727  
728  
729  
730  
731  
732  
733  
734  
735  
736  
737  
738  
739  
740  
741  
742  
743  
744  
745  
746  
747  
748  
749  
750  
751  
752  
753  
754  
755  
756  
757  
758  
759  
760  
761  
762  
763  
764  
765  
766  
767  
768  
769  
770  
771  
772  
773  
774  
775  
776  
777  
778  
779  
780  
781  
782  
783  
784  
785  
786  
787  
788  
789  
790  
791  
792  
793  
794  
795  
796  
797  
798  
799  
800  
801  
802  
803  
804  
805  
806  
807  
808  
809  
810  
811  
812  
813  
814  
815  
816  
817  
818  
819  
820  
821  
822  
823  
824  
825  
826  
827  
828  
829  
830  
831  
832  
833  
834  
835  
836  
837  
838  
839  
840  
841  
842  
843  
844  
845  
846  
847  
848  
849  
850  
851  
852  
853  
854  
855  
856  
857  
858  
859  
860  
861  
862  
863  
864  
865  
866  
867  
868  
869  
870  
871  
872  
873  
874  
875  
876  
877  
878  
879  
880  
881  
882  
883  
884  
885  
886  
887  
888  
889  
890  
891  
892  
893  
894  
895  
896  
897  
898  
899  
900  
901  
902  
903  
904  
905  
906  
907  
908  
909  
910  
911  
912  
913  
914  
915  
916  
917  
918  
919  
920  
921  
922  
923  
924  
925  
926  
927  
928  
929  
930  
931  
932  
933  
934  
935  
936  
937  
938  
939  
940  
941  
942  
943  
944  
945  
946  
947  
948  
949  
950  
951  
952  
953  
954  
955  
956  
957  
958  
959  
960  
961  
962  
963  
964  
965  
966  
967  
968  
969  
970  
971  
972  
973  
974  
975  
976  
977  
978  
979  
980  
981  
982  
983  
984  
985  
986  
987  
988  
989  
990  
991  
992  
993  
994  
995  
996  
997  
998  
999  
1000  
1001  
1002  
1003  
1004  
1005  
1006  
1007  
1008  
1009  
1010  
1011  
1012  
1013  
1014  
1015  
1016  
1017  
1018  
1019  
1020  
1021  
1022  
1023  
1024  
1025  
1026  
1027  
1028  
1029  
1030  
1031  
1032  
1033  
1034  
1035  
1036  
1037  
1038  
1039  
1040  
1041  
1042  
1043  
1044  
1045  
1046  
1047  
1048  
1049  
1050  
1051  
1052  
1053  
1054  
1055  
1056  
1057  
1058  
1059  
1060  
1061  
1062  
1063  
1064  
1065  
1066  
1067  
1068  
1069  
1070  
1071  
1072  
1073  
1074  
1075  
1076  
1077  
1078  
1079  
1080  
1081  
1082  
1083  
1084  
1085  
1086  
1087  
1088  
1089  
1090  
1091  
1092  
1093  
1094  
1095  
1096  
1097  
1098  
1099  
1100  
1101  
1102  
1103  
1104  
1105  
1106  
1107  
1108  
1109  
1110  
1111  
1112  
1113  
1114  
1115  
1116  
1117  
1118  
1119  
1120  
1121  
1122  
1123  
1124  
1125  
1126  
1127  
1128  
1129  
1130  
1131  
1132  
1133  
1134  
1135  
1136  
1137  
1138  
1139  
1140  
1141  
1142  
1143  
1144  
1145  
1146  
1147  
1148  
1149  
1150  
1151  
1152  
1153  
1154  
1155  
1156  
1157  
1158  
1159  
1160  
1161  
1162  
1163  
1164  
1165  
1166  
1167  
1168  
1169  
1170  
1171  
1172  
1173  
1174  
1175  
1176  
1177  
1178  
1179  
1180  
1181  
1182  
1183  
1184  
1185  
1186  
1187  
1188  
1189  
1190  
1191  
1192  
1193  
1194  
1195  
1196  
1197  
1198  
1199  
1200  
1201  
1202  
1203  
1204  
1205  
1206  
1207  
1208  
1209  
1210  
1211  
1212  
1213  
1214  
1215  
1216  
1217  
1218  
1219  
1220  
1221  
1222  
1223  
1224  
1225  
1226  
1227  
1228  
1229  
1230  
1231  
1232  
1233  
1234  
1235  
1236  
1237  
1238  
1239  
1240  
1241  
1242  
1243  
1244  
1245  
1246  
1247  
1248  
1249  
1250  
1251  
1252  
1253  
1254  
1255  
1256  
1257  
1258  
1259  
1260  
1261  
1262  
1263  
1264  
1265  
1266  
1267  
1268  
1269  
1270  
1271  
1272  
1273  
1274  
1275  
1276  
1277  
1278  
1279  
1280  
1281  
1282  
1283  
1284  
1285  
1286  
1287  
1288  
1289  
1290  
1291  
1292  
1293  
1294  
1295  
1296  
1297  
1298  
1299  
1300  
1301  
1302  
1303  
1304  
1305  
1306  
1307  
1308  
1309  
1310  
1311  
1312  
1313  
1314  
1315  
1316  
1317  
1318  
1319  
1320  
1321  
1322  
1323  
1324  
1325  
1326  
1327  
1328  
1329  
1330  
1331  
1332  
1333  
1334  
1335  
1336  
1337  
1338  
1339  
1340  
1341  
1342  
1343  
1344  
1345  
1346  
1347  
1348  
1349  
1350  
1351  
1352  
1353  
1354  
1355  
1356  
1357  
1358  
1359  
1360  
1361  
1362  
1363  
1364  
1365  
1366  
1367  
1368  
1369  
1370  
1371  
1372  
1373  
1374  
1375  
1376  
1377  
1378  
1379  
1380  
1381  
1382  
1383  
1384  
1385  
1386  
1387  
1388  
1389  
1390  
1391  
1392  
1393  
1394  
1395  
1396  
1397  
1398  
1399  
1400  
1401  
1402  
1403  
1404  
1405  
1406  
1407  
1408  
1409  
1410  
1411  
1412  
1413  
1414  
1415  
1416  
1417  
1418  
1419  
1420  
1421  
1422  
1423  
1424  
1425  
1426  
1427  
1428  
1429  
1430  
1431  
1432  
1433  
1434  
1435  
1436  
1437  
1438  
1439  
1440  
1441  
1442  
1443  
1444  
1445  
1446  
1447  
1448  
1449  
1450  
1451  
1452  
1453  
1454  
1455  
1456  
1457  
1458  
1459  
1460  
1461  
1462  
1463  
1464  
1465  
1466  
1467  
1468  
1469  
1470  
1471  
1472  
1473  
1474  
1475  
1476  
1477  
1478  
1479  
1480  
1481  
1482  
1483  
1484  
1485  
1486  
1487  
1488  
1489  
1490  
1491  
1492  
1493  
1494  
1495  
1496  
1497  
1498  
1499  
1500  
1501  
1502  
1503  
1504  
1505  
1506  
1507  
1508  
1509  
1510  
1511  
1512  
1513  
1514  
1515  
1516  
1517  
1518  
1519  
1520  
1521  
1522  
1523  
1524  
1525  
1526  
1527  
1528  
1529  
1530  
1531  
1532  
1533  
1534  
1535  
1536  
1537  
1538  
1539  
1540  
1541  
1542  
1543  
1544  
1545  
1546  
1547  
1548  
1549  
1550  
1551  
1552  
1553  
1554  
1555  
1556  
1557  
1558  
1559  
1560  
1561  
1562  
1563  
1564  
1565  
1566  
1567  
1568  
1569  
1570  
1571  
1572  
1573  
1574  
1575  
1576  
1577  
1578  
1579  
1580  
1581  
1582  
1583  
1584  
1585  
1586  
1587  
1588  
1589  
1590  
1591  
1592  
1593  
1594  
1595  
1596  
1597  
1598  
1599  
1600  
1601  
1602  
1603  
1604  
1605  
1606  
1607  
1608  
1609  
1610  
1611  
1612  
1613  
1614  
1615  
1616  
1617  
1618  
1619  
1620  
1621  
1622  
1623  
1624  
1625  
1626  
1627  
1628  
1629  
1630  
1631  
1632  
1633  
1634  
1635  
1636  
1637  
1638  
1639  
1640  
1641  
1642  
1643  
1644  
1645  
1646  
1647  
1648  
1649  
1650  
1651  
1652  
1653  
1654  
1655  
1656  
1657  
1658  
1659  
1660  
1661  
1662  
1663  
1664  
1665  
1666  
1667  
1668  
1669  
1670  
1671  
1672  
1673  
1674  
1675  
1676  
1677  
1678  
1679  
1680  
1681  
1682  
1683  
1684  
1685  
1686  
1687  
1688  
1689  
1690  
1691  
1692  
1693  
1694  
1695  
1696  
1697  
1698  
1699  
1700  
1701  
1702  
1703  
1704  
1705  
1706  
1707  
1708  
1709  
1710  
1711  
1712  
1713  
1714  
1715  
1716  
1717  
1718  
1719  
1720  
1721  
1722  
1723  
1724  
1725  
1726  
1727  
1728  
1729  
1730  
1731  
1732  
1733  
1734  
1735  
1736  
1737  
1738  
1739  
1740  
1741  
1742  
1743  
1744  
1745  
1746  
1747  
1748  
1749  
1750  
1751  
1752  
1753  
1754  
1755  
1756  
1757  
1758  
1759  
1760  
1761  
1762  
1763  
1764  
1765  
1766  
1767  
1768  
1769  
1770  
1771  
1772  
1773  
1774  
1775  
1776  
1777  
1778  
1779  
1780  
1781  
1782  
1783  
1784  
1785  
1786  
1787  
1788  
1789  
1790  
1791  
1792  
1793  
1794  
1795  
1796  
1797  
1798  
1799  
1800  
1801  
1802  
1803  
1804  
1805  
1806  
1807  
1808  
1809  
1810  
1811  
1812  
1813  
1814  
1815  
1816  
1817  
1818  
1819  
1820  
1821  
1822  
1823  
1824  
1825  
1826  
1827  
1828  
1829  
1830  
1831  
1832  
1833  
1834  
1835  
1836  
1837  
1838  
1839  
1840  
1841  
1842  
1843  
1844  
1845  
1846  
1847  
1848  
1849  
1850  
1851  
1852  
1853  
1854  
1855  
1856  
1857  
1858  
1859  
1860  
1861  
1862  
1863  
1864  
1865  
1866  
1867  
1868  
1869  
1870  
1871  
1872  
1873  
1874  
1875  
1876  
1877  
1878  
1879  
1880  
1881  
1882  
1883  
1884  
1885  
1886  
1887  
1888  
1889  
1890  
1891  
1892  
1893  
1894  
1895  
1896  
1897  
1898  
1899  
1900  
1901  
1902  
1903  
1904  
1905  
1906  
1907  
1908  
1909  
1910  
1911  
1912  
1913  
1914  
1915  
1916  
1917  
1918  
1919  
1920  
1921  
1922  
1923  
1924  
1925  
1926  
1927  
1928  
1929  
1930  
1931  
1932  
1933  
1934  
1935  
1936  
1937  
1938  
1939  
1940  
1941  
1942  
1943  
1944  
1945  
1946  
1947  
1948  
1949  
1950  
1951  
1952  
1953  
1954  
1955  
1956  
1957  
1958  
1959  
1960  
1961  
1962  
1963  
1964  
1965  
1966  
1967  
1968  
1969  
1970  
1971  
1972  
1973  
1974  
1975  
1976  
1977  
1978  
1979  
1980  
1981  
1982  
1983  
1984  
1985  
1986  
1987  
1988  
1989  
1990  
1991  
1992  
1993  
1994  
1995  
1996  
1997  
1998  
1999  
2000  
2001  
2002  
2003  
2004  
2005  
2006  
2007  
2008  
2009  
2010  
2011  
2012  
2013  
2014  
2015  
2016  
2017  
2018  
2019  
2020  
2021  
2022  
2023  
2024  
2025  
2026  
2027  
2028  
2029  
2030  
2031  
2032  
2033  
2034  
2035  
2036  
2037  
2038  
2039  
2040  
2041  
2042  
2043  
2044  
2045  
2046  
2047  
2048  
2049  
2050  
2051  
2052  
2053  
2054  
2055  
2056  
2057  
2058  
2059  
2060  
2061  
2062  
2063  
2064  
2065  
2066  
2067  
2068  
2069  
2070  
2071  
2072  
2073  
2074  
2075  
2076  
2077  
2078  
2079  
2080  
2081  
2082  
2083  
2084  
2085  
2086  
2087  
2088  
2089  
2090  
2091  
2092  
2093  
2094  
2095  
2096  
2097  
2098  
2099  
2100  
2101  
2102  
2103  
2104  
2105  
2106  
2107  
2108  
2109  
2110  
2111  
2112  
2113  
2114  
2115  
2116  
2117  
2118  
2119  
2120  
2121  
2122  
2123  
2124  
2125  
2126  
2127  
2128  
2129  
2130  
2131  
2132  
2133  
2134  
2135  
2136  
2137  
2138  
2139  
2140  
2141  
2142  
2143  
2144  
2145  
2146  
2147  
2148  
2149  
2150  
2151  
2152  
2153  
2154  
2155  
2156  
2157  
2158  
2159  
2160  
2161

FABRICATION OF MICROWAVE WAVE GUIDES  
 USING  
 HIGH T<sub>c</sub> SUPERCONDUCTORS  
 Final Report - Table of Contents

	PAGE #
1.0 Introduction . . . . .	3
2.0 Experimental . . . . .	4
3.0 Results and Discussion . . . . .	7
4.0 Conclusion . . . . .	29
5.0 Acknowledgments . . . . .	29
6.0 References . . . . .	30
Appendix A . . . . .	31

NO INVENTIONS DISCLOSED



Approved For	
CRS - CRA&I	J
CRIC - TAB	U
Unannounced	U
Justification	
By	
Distribution /	
Availability Codes	
Dist	Approved for Special
A-1	

## 1.0. INTRODUCTION

The objective of this study was to produce bulk high  $T_c$  superconductor  $YBa_2Cu_3O_{7-x}$  with microwave conductivity at least as good or better than that of copper. The subsequent aim was to fabricate cylindrical wave guide using this material. The ultimate goal of this study is to produce  $YBa_2Cu_3O_{7-x}$  with microwave conductivity exceedingly higher (at least two orders of magnitude better) than that of copper. In principle, this is possible if the microstructure of the superconductor material is carefully controlled.

The above-stated goal could be easily achieved if the large single crystals of  $YBa_2Cu_3O_{7-x}$  are available or if the inside surface of a suitable substrate material in the form of hollow cylinder, could be coated with the superconductor material of high quality. The former approach, currently, seems to be far from practical realization. A great deal of work on producing high quality epitaxial films of  $YBa_2Cu_3O_{7-x}$  has been and is being carried out at a number of academic and industrial institutions. However, to the best of our knowledge, practical utilization of thin film high  $T_c$  superconductors to fabricate microwave wave guide has not been achieved so far. Therefore, in the present work the alternative to produce bulk  $YBa_2Cu_3O_{7-x}$  with microwave characteristics comparable to or better than that of copper was selected. At microwave frequencies, the electromagnetic waves do not penetrate in a conductor to a great extent (due to skin effect), and conduction takes place mainly at the surface. Hence, the integrity of the superconductor surface is of great importance. At present all the thin films and bulk superconductor materials are produced in a polycrystalline form only. Therefore, the grain to grain interconnect over the surface is very essential. In order to achieve this goal, the work was focused at the following specific points:

1. Optimization of the process parameters to obtain reproducible  $YBa_2Cu_3O_{7-x}$  with  $T_c > 90^{\circ}K$ .
2. To obtain  $YBa_2Cu_3O_{7-x}$  with largest possible grains with better grain to grain interconnect.
3. To study the effect of the addition of gold to improve the grain to grain interconnect.

It was found during the present study that for the fixed time, the oxygen annealing temperature was the limiting factor for the grain size. Also, addition of the optimum amount of gold to  $YBa_2Cu_3O_{7-x}$  not only improved the  $T_c$  of the material, but also increases the grain size. To the best of the authors' knowledge, this favorable effect of gold has not been reported in the U.S. open literature and is reported here for the first

time. Detailed study of the effect of the addition of gold to  $\text{YBa}_2\text{Cu}_3\text{O}_{7-x}$  needs further research. The microwave conductivity measurements were carried out at the COMSAT laboratories with the help of Dr. Andrew Meulenberg. Microwave conductivity was determined by measuring the quality factor,  $Q$ , of a reflecting resonance cavity operating in  $\text{TE}_{011}$  mode. At about 16 GHz and 77°K conductivity of gold mixed  $\text{YBa}_2\text{Cu}_3\text{O}_{7-x}$  was found to be about the same as that of copper. For superconductor material, the conductivity varies as the inverse of square of the frequency. This means at 8 GHz this superconductor material has conductivity about 4 times better than that of copper.

## 2.0 EXPERIMENTAL

2.1 Synthesis of high  $T_C$   $\text{YBa}_2\text{Cu}_3\text{O}_{7-x}$ : During the present study the samples were synthesized from high purity  $\text{Y}_2\text{O}_3$  (99-999%),  $\text{BaCO}_3$  (99-997%), and  $\text{CuO}$  (99-999%) supplied by AESAR (Johnson Matthey). The stoichiometric mixture of these three oxides was ground and mixed in agate mortar and pestle. Thin pallets were formed from this mixture using stainless steel dies and hydraulic press. Pallets of two diameters, i.e. 0.75" and 0.50" in the thickness range of 2.5mm to 8mm were made during this study. These pallets were calcinated at 950°C in a  $\text{O}_2$  environment using a computer controlled furnace for about 18 hours. The reacted material samples were then removed from the furnace and then ground in mortar and pestle. Using this powder, the pallets were formed by compression. In case the initial pallets were thicker than 4mm, the material was once again reacted under the same condition to ensure the proper composition and stoichiometry of the resulting material. The stoichiometry of the powder/pallets was also checked by x-ray diffraction. Once the formation of the stoichiometric material was ensured, the next step was the oxygen annealing of samples in the pallet forms. The pallets were made from presynthesized  $\text{YBa}_2\text{Cu}_3\text{O}_{7-x}$  by compression in a pressure range 3.5kbar to 9.5kbar. During the oxygen annealing material was cooled to room temperature at the rate of 2°C/min. To study the effect of the addition of gold during the present work,  $\text{YBa}_2\text{Cu}_3\text{O}_{7-x}$  samples containing 10% by weight and 20% by weight of gold were prepared. High  $T_C$   $\text{YBa}_2\text{Cu}_3\text{O}_{7-x}$  powder and required amount of 99.95% pure gold flakes (1-3µm particle size) were mixed in a dry bottle. The mixture of these powders was then used for making pallets by compression and were subsequently oxygen annealed. For making cylinders of high  $T_C$   $\text{YBa}_2\text{Cu}_3\text{O}_{7-x}$ , a special stainless steel die set was made. This die set can make cylinders with length up to 1 inch and outer and inner diameters of 0.75 inch and 0.50 inch, respectively.

2.2 X-ray diffraction using a curved position sensitive detector: To identify and ascertain the superconducting phase in the specimen prepared by the above-mentioned method, x-ray diffraction method was used. The experimental system in the present work consisted of the following major components:

1. GE XRD-7 x-ray generator with CA8-F/Cu x-ray tube,
2. Spectrogoniometer,
3. Silicon crystal monochromator,
4. Sample holder, and
5. Curved Position Sensitive Detector (CPSD) with data acquisition analysis and storage accessories.

The schematic of the experimental system is shown in Figure 1. As opposed to the conventional diffractometric system, the CPSD used for this work is a novel x-ray detector. It has an angular range of  $120^\circ$  and diffraction peaks/lines in this range can be simultaneously obtained without moving the detector. A special holder to mount the CPSD on the spectrometer was fabricated. A detailed description of the CPSD and the calibration procedure is given in Appendix A.

2.3 D.C. resistivity measurements: Resistivity measurements were done using four probe techniques. Contacts were made using thin copper wires and silver paint. Keithley 197 autoranging microvoltmeter, Keithley 224 programmable constant current source, and Keithley 740 system scanning thermometer were used along with IBM PC for these measurements. The sample was cooled to liquid nitrogen temperature and was allowed to warm-up in a natural fashion. A constant current of 1mA and 10mA were applied, and the voltage was measured using a microvoltmeter at various temperatures. The data collected by the personal computer were graphically plotted as relative resistivity versus temperature.

2.4 Microwave conductivity: Microwave conductivity of the superconducting samples have been determined at COMSAT Laboratories with the help of Dr. Meulenberg. The measurements on superconductor as well as copper samples of the same dimensions were made at liquid nitrogen temperature. Microwave conductivity was determined by measuring the quality factor,  $Q$ , of a reflecting resonance cavity operating in  $TE_{011}$  mode. Results for a cavity having an endplate replaced with the sample were referenced against those for a cavity with an absorbing endplate. The  $Q$  of a cavity is determined [1,2] by measuring the loss in reflected power at resonance, calculating the level at half maximum (or some other fixed percentage level), and interpolating between data points to determine the frequencies corresponding to this level. The value obtained from the center frequency ( $f_c$ ) divided by the frequency difference between the half-maximum points ( $\Delta f$ ) is the loaded  $Q$  ( $Q_L$ ) of the system.

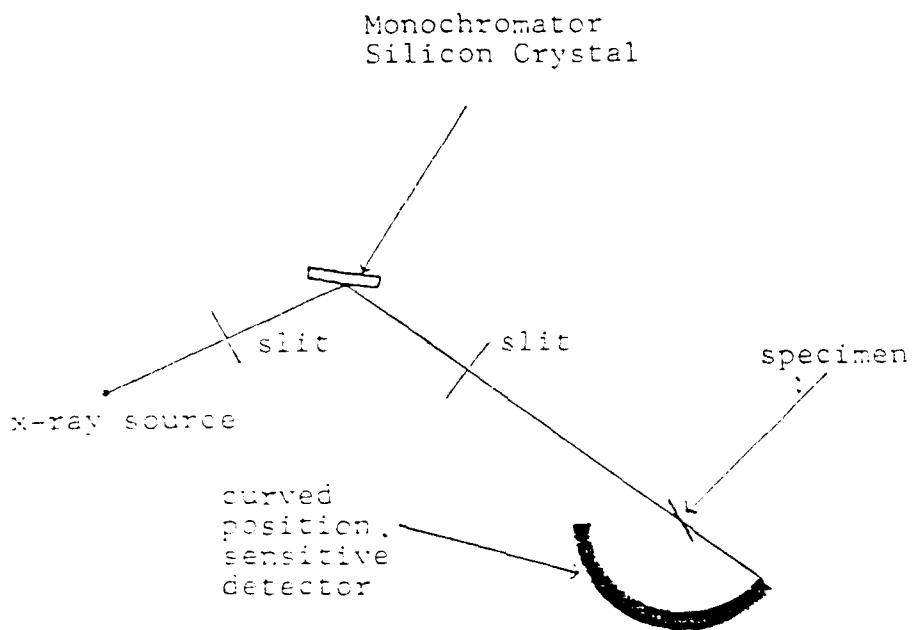


Figure 1. Schematic illustrating the experimental diffraction system.

2.5 Optical microscopy: The microstructure of the samples was studied using an Olympus inverted metallurgical microscope (Model PME). Samples were observed with both the normal and polarized light. A superconductor phase can be normally identified by the presence of twins in the grain when viewed using polarized light. The photographs revealing the microstructure of samples were taken using polaroid type 55 films.

### 3.0 RESULTS AND DISCUSSION

The synthesis of superconducting  $\text{YBa}_2\text{Cu}_3\text{O}_{7-x}$  involve two major steps.

1. Calcination of the starting ingredients (i.e.  $\text{Y}_2\text{O}_3$ ,  $\text{BaCO}_3$  and  $\text{CuO}$ ) to obtain the stoichiometric  $\text{YBa}_2\text{Cu}_3\text{O}_{7-x}$ .
2. Oxygen annealing of the stoichiometric phase where slow cooling of the sample from the annealing temperature is very essential to obtain superconducting phase.

These steps involve the following material/process parameters.

1. The purity of starting ingredients.
2. Pressure used for the compression of pallets.
3. Particle size distribution in the material to be compressed.
4. Calcination and oxygen annealing temperatures.
5. Calcination and oxygen annealing time.  
and
6. The rate of cooling (after oxygen annealing).

During the entire course of the reported study the highest purity materials available were used. The oxygen annealing was carried out at 650-700 Torr. This oxygen pressure range was determined to be optimum. The calcination temperature used during this study was  $950^\circ\text{C}$  and was kept constant during the entire study.

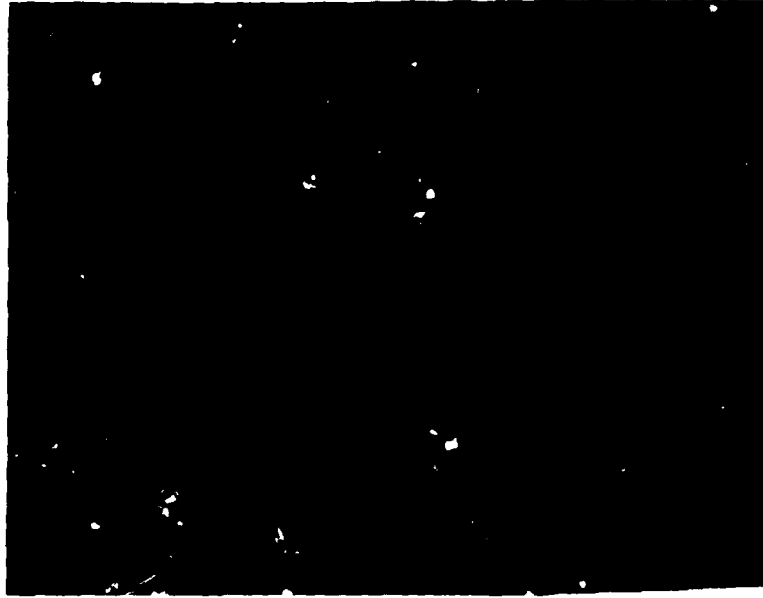
When pallets of  $\text{YBa}_2\text{Cu}_3\text{O}_{7-x}$  powder were made for oxygen annealing, the particle size distribution in the powder did not seem to have any effect on the transition temperature. However, the powder containing smaller particles required higher pressure for the pallet compression. The void density and void size in the pallets made from smaller particles were less as compared to those in pallets made from larger particles. These effects are illustrated in Figures 2(a) and 2(b). The photograph in Figure 2(a) shows the microstructure of the surface of the pallet made from the powder having

particle size in the range of 44 $\mu$ m - 74 $\mu$ m. The sample shown in Figure 2(b) contained particles in the size range of 74 $\mu$ m - 149 $\mu$ m. Figures 3(a) and 3(b) show the four probe D.C. resistivity measurements on the pallets in Figure 2(a) and 2(b), respectively. Both samples show  $T_c$  onset of 95°K with zero resistivity at 90°K. The data scatter in these initial measurements is due to using a low applied current (1mA) and, therefore, the digital microvoltmeter at the lower limit of resolution.

The effect of the pressure (during compression of the pallets) was studied during in the initial period of this work. Pressures in the range 3.5kbar to 9.5kbar were used. In this range the pressure did not have significant effect on the transition temperature. However, the packing density of the compacted material changed significantly. For 5mm thick pallet the packing density varied from about 48% at 3.5kbar to about 81% at 9.5kbar. Figures 4(a), 4(b) and 5(a), 5(b) illustrates the effect of pressure on the microstructure. Figure 4(a) is a microphotograph of a surface of the pallet compressed at 3.5kbar. Figure 4(b) is the microphotograph of the surface of the same pallet after oxygen annealing at 960°C. Figure 5(a) and 5(b) are the microphotographs of the pallet compressed at 9.5kbar surface before and after the oxygen annealing at 960°C. For both samples, the particle size distribution of the starting  $YBa_2Cu_3O_{7-x}$  powder was the same. After compression, the pallet compressed at higher pressure (9.5kbar) has relatively much smaller particle/grain sizes. After oxygen annealing, both samples have the same average grain size. However in a sample which was compressed at 9.5kbar, the grain to grain interconnect is much better and the density of voids and "unfaceted" phase is lower than that in the pallet compressed at 3.5kbar. Figure 6(a) and 6(b) show results of the D.C. resistivity measurements of these samples. These results indicate that they have the same transition temperatures. At this time, we do not know if the "unfaceted" phase in the sample surface mentioned earlier is also superconducting. It is required to further study this unfaceted phase using electron microscopy and electron microprobe analysis techniques. The packing density and, hence, the pressure will be of critical importance when it is required to transmit a very high current density through the bulk of a sample.

(X800)

(a)



(b)



Figure 2 Microstructure of  $\text{YBa}_2\text{Cu}_3\text{O}_{7-x}$  pallets prepared using the powder with particles in the size range (a) 44 - 74 $\mu\text{m}$  and (b) 74 - 149 $\mu\text{m}$ , respectively.

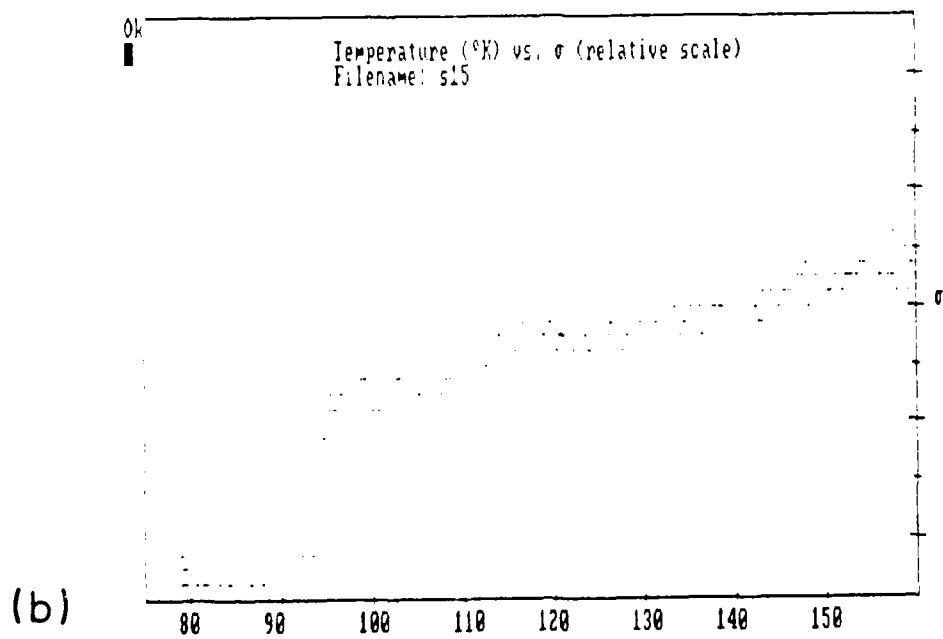
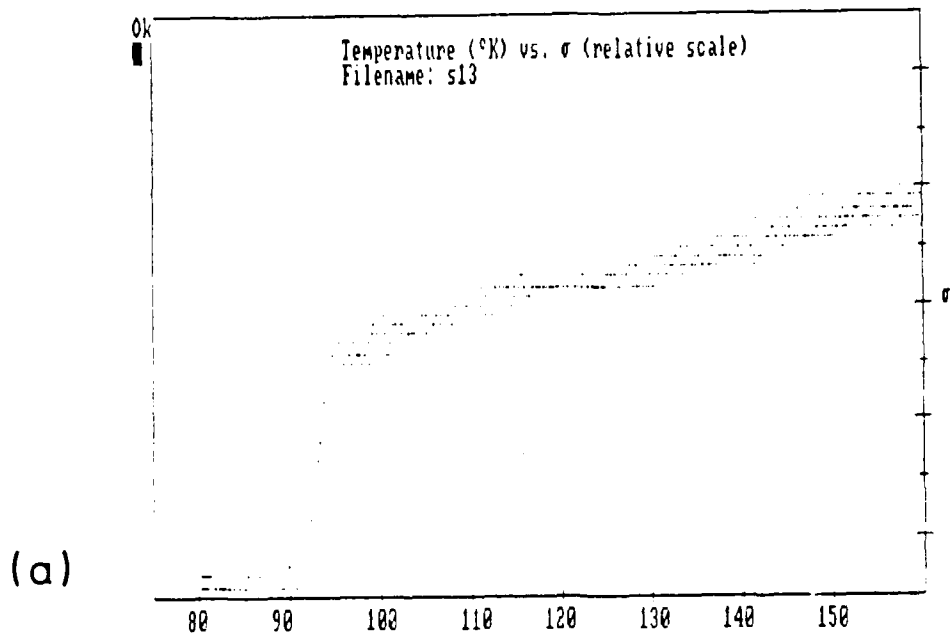
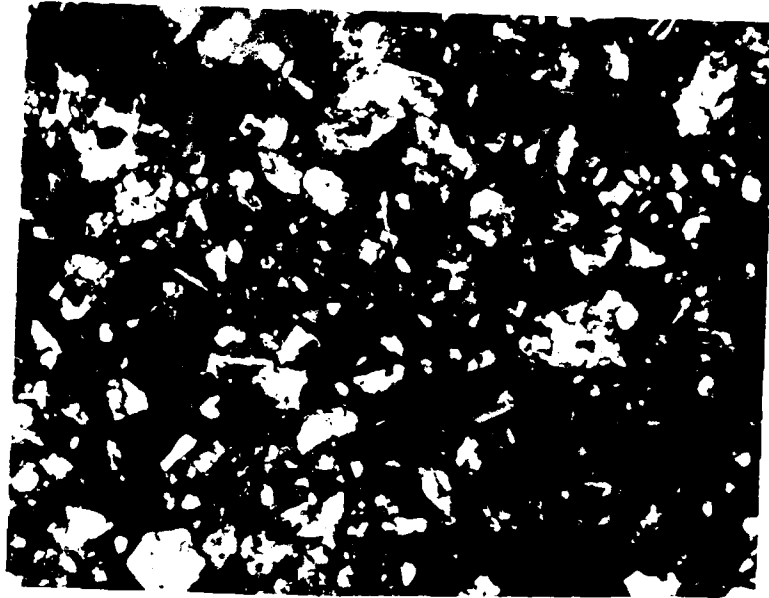


Figure 3 D.C. resistivity measurements on the  $\text{YBa}_2\text{Cu}_3\text{O}_{7-x}$  prepared using the powder with particle size distribution in the range (a) 44 - 74 $\mu\text{m}$  and (b) 74 - 149 $\mu\text{m}$ .

(X800)

(a)



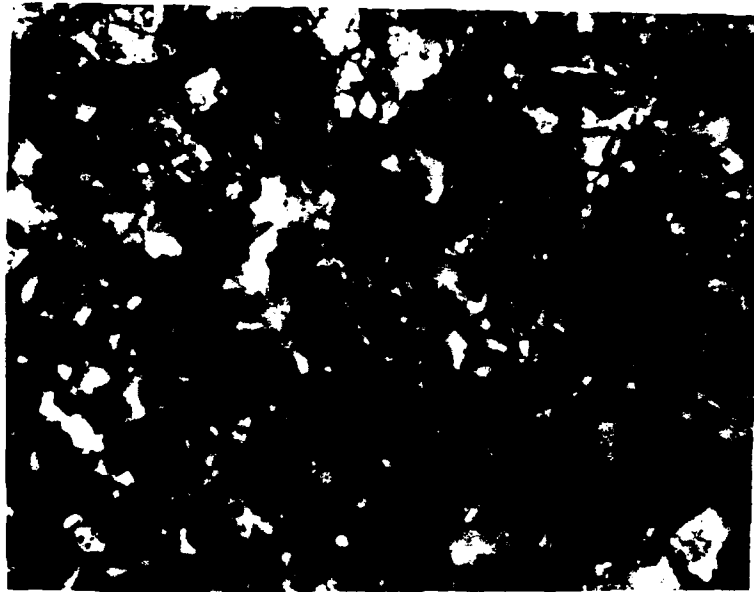
(b)



Figure 4 Micro-photograph showing the microstructure of  $\text{YBa}_2\text{Cu}_3\text{O}_{7-x}$  pallet compacted using the pressure of 3.5kbar (a) before (b) after oxygen annealing.

(X800)

(a)

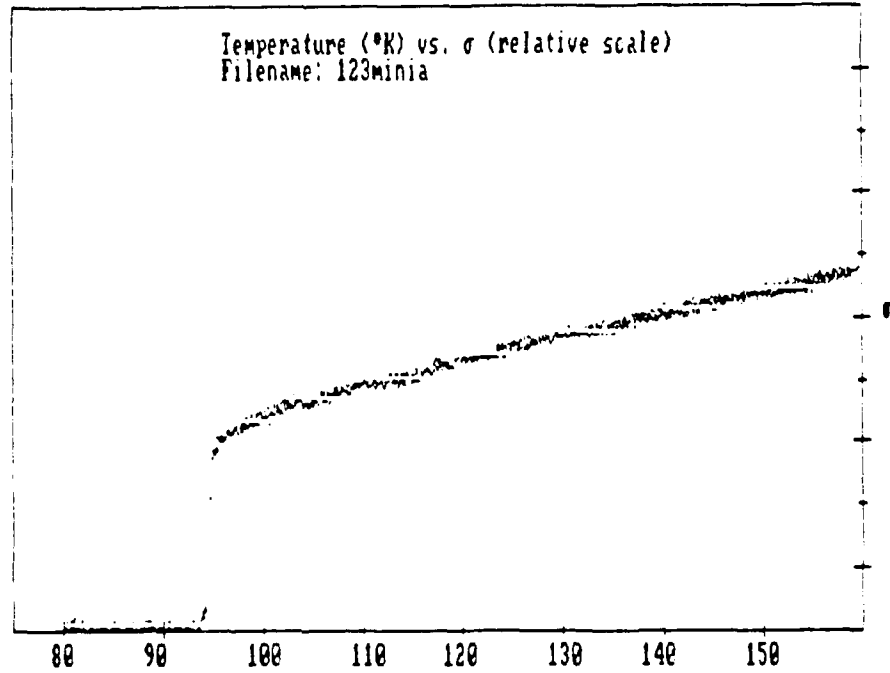


(b)



Figure 5 Photograph showing the microstructure of  $\text{YBa}_2\text{Cu}_3\text{O}_{7-x}$  pallet compacted using the pressure of 9.5kbar (a) before and (b) after oxygen annealing.

(a)



(b)

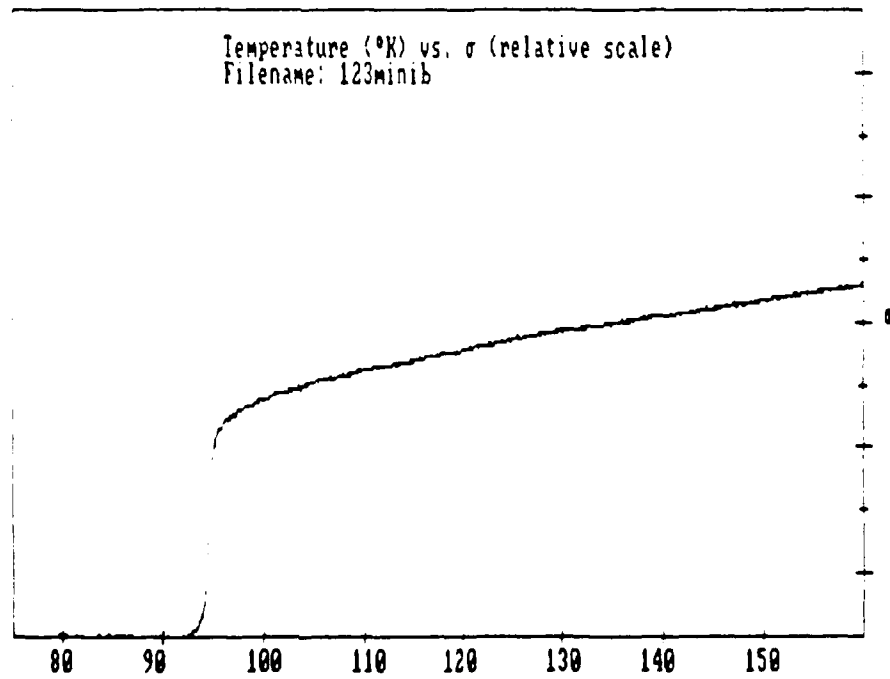


Figure 6 D.C. resistivity measurements on  $\text{YBa}_2\text{Cu}_3\text{O}_{7-x}$  pallets prepared using (a) 3.5kbar and (b) 9.5kbar pressure, respectively.

The effect of temperature on the microstructure during oxygen annealing was studied at three different temperatures of 945°C, 960°C, and 975°C. Above 975°C  $\text{YBa}_2\text{Cu}_3\text{O}_{7-x}$  is believed to decompose and phase separation takes place resulting into Ba and Cu poor material [3]. As expected in sintering process the grain size was found to increase with increasing temperature. Figures 7(a), 7(b), and 7(c) show the microstructure of the samples oxygen annealed at 945°C (sample A), 960°C (sample B), and 975°C (sample C). In Figure 7(a) a fine network of small faceted grains (1-6µm) separated by unfaceted regions and voids can be seen. Compared to Figure 7(a) in Figure 7(b) a significant increase in grain size is obvious. Grains as large as 50-60µm were observed. At the same time the size of unfaceted phase and voids also increased in size as compared to those in specimen in Figure 7(a). In Figure 7(c), which is a microphotograph of a surface of the specimen annealed at 975°C, the largest grain size among the specimen studied here is observed. Most of the grains in this sample are separated by the unfaceted phase or voids. The composition of the three samples discussed above was checked using x-ray diffraction. X-ray diffraction patterns of these sample area shown in Figures 8(a), 8(b), and 8(c) are in good general agreement with earlier reported [4] patterns for  $\text{YBa}_2\text{Cu}_3\text{O}_{7-x}$ . The D.C. resistivity data of these samples are presented in Figure 9(a), 9(b), and 9(c) which shows the superconducting transition temperature onset at about 96°K, 94°K, and 93.8°K respectively. However, the zero resistivity is observed at about 93.8°K in Figure 9(a) and at about 92.5°K for samples with data in Figure 9(b) and 9(c), respectively. The transition width is minimum for the samples containing largest grains (i.e. Figure 9(c)). The microwave measurement data on these samples are shown in Table I.

As mentioned earlier microwave measurements involved measurement of quality factor  $Q$  of a reflecting resonance cavity in  $\text{TE}_{011}$  mode. The  $Q$  of cavity is easy to measure and can be determined using the relation:  $Q = \text{center frequency}/3\text{db bandwidth}$ . In the present case  $Q$  for the cavity having an endplate replaced with the superconductor sample were referenced against those for a cavity with a copper end plate. In this configuration the surface resistance of a superconductor sample can be determined using the following expression:  $R = \text{geometric factor} \times (1/Q_{\text{Cu}} - 1/Q_{\text{S}})$  where  $Q_{\text{Cu}}$  is the quality factor of the cavity with copper as endplate and  $Q_{\text{S}}$  is the qualifactor of the cavity wish superconductor sample as an endplate.

Now let us consider the results in Table I. At liquid nitrogen temperature the material with the largest grain size has  $Q/Q_{Cu} = 0.91$ . To first approximation we can say that conductivity of this sample at  $77^{\circ}\text{K}$  and about 16 GHz is 91%

TABLE I

SAMPLE	TEMP	$C_f$ (GHz)	$\Delta_f$ (MHz)	$Q = C_f/\Delta_f$ (x1000)	n	$Q_s/Q_{Cu}$
copper	RT	15.434	1.2	12.86	0.5	--
copper	LN <sub>2</sub>	15.491	0.6	25.82	0.5	--
A	RT	15.644	3.8	4.12	2.5	0.32
A	LN <sub>2</sub>	15.701	0.8	19.63	.55	0.76
B	RT	15.220	2.8	5.43	1	42.2
B	LN <sub>2</sub>	15.270	0.7	21.8	2	0.84
C	RT	15.223	2.6	5.85	2.8	0.45
C	LN <sub>2</sub>	15.269	0.65	23.49	0.8	0.91

$C_f$  - Center Frequency

$\Delta_f$  - Frequency Bandwidth

n - Coupling Coefficient

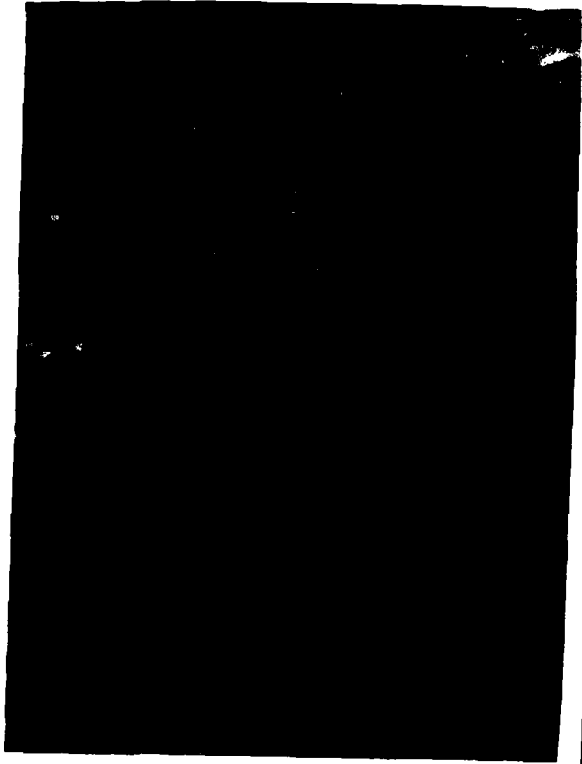
$Q_s/Q_{Cu}$  - Ratio of the quality factor of cavity with superconductor as endplate to quality factor of the cavity with copper as endplate. This ratio for each sample is calculated at room temperature and liquid nitrogen temperature.

RT - Room Temperature (about  $300^{\circ}\text{K}$ )

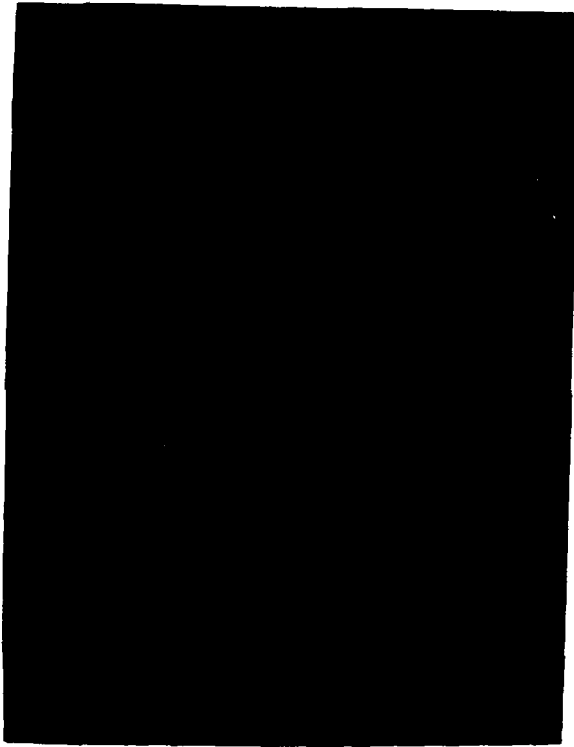
LN<sub>2</sub> - Liquid Nitrogen Temperature ( $77^{\circ}\text{K}$ )



(a)



(b)



(c)

(X800)

Figure 7 Photographs showing the microstructure of  $\text{YBa}_2\text{Cu}_3\text{O}_{7-x}$  samples processed at (a)  $945^\circ\text{C}$  (sample A), (b)  $960^\circ\text{C}$  (sample B), and (c)  $975^\circ\text{C}$  (sample C), respectively. Increase in grain size with increasing processing temperature can be easily observed in these photographs.

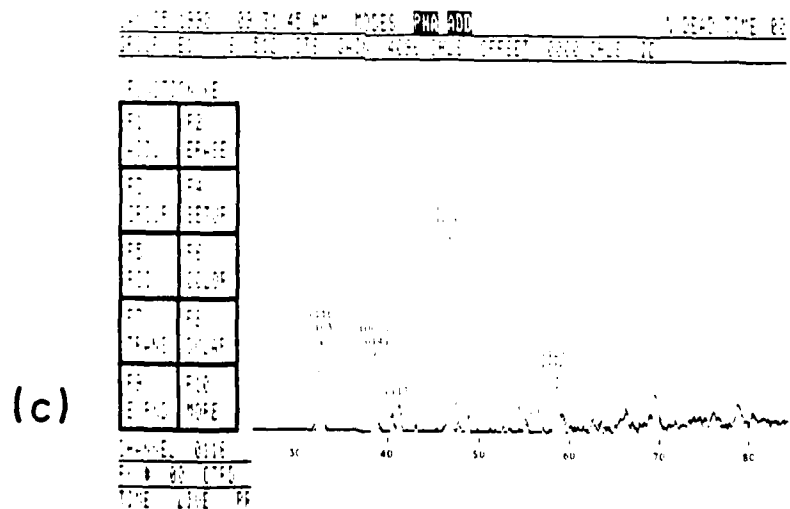
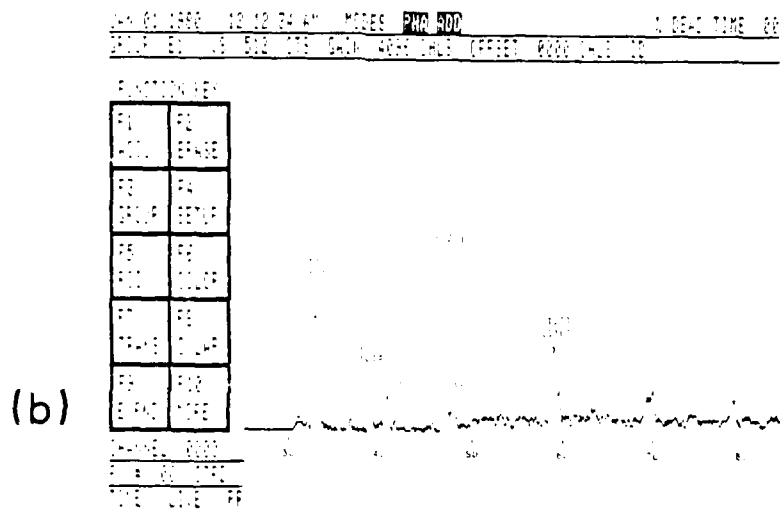
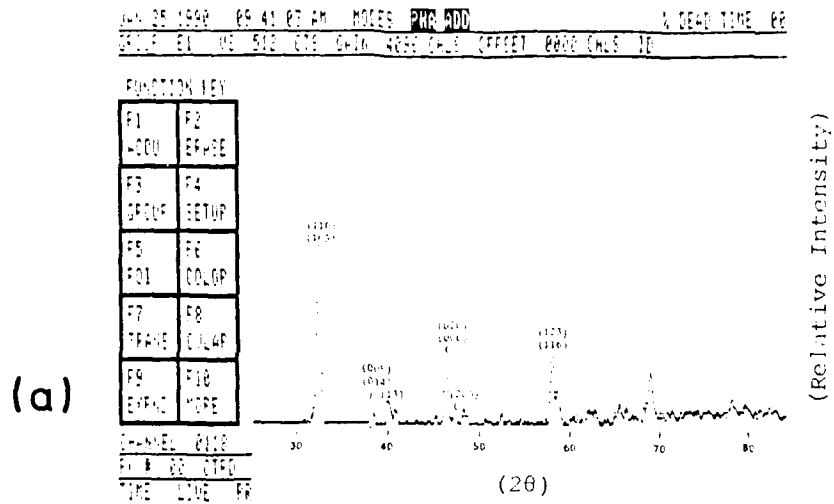


Figure 8 X-ray diffraction patterns of (a) sample A, (b) sample B, and (c) sample C.

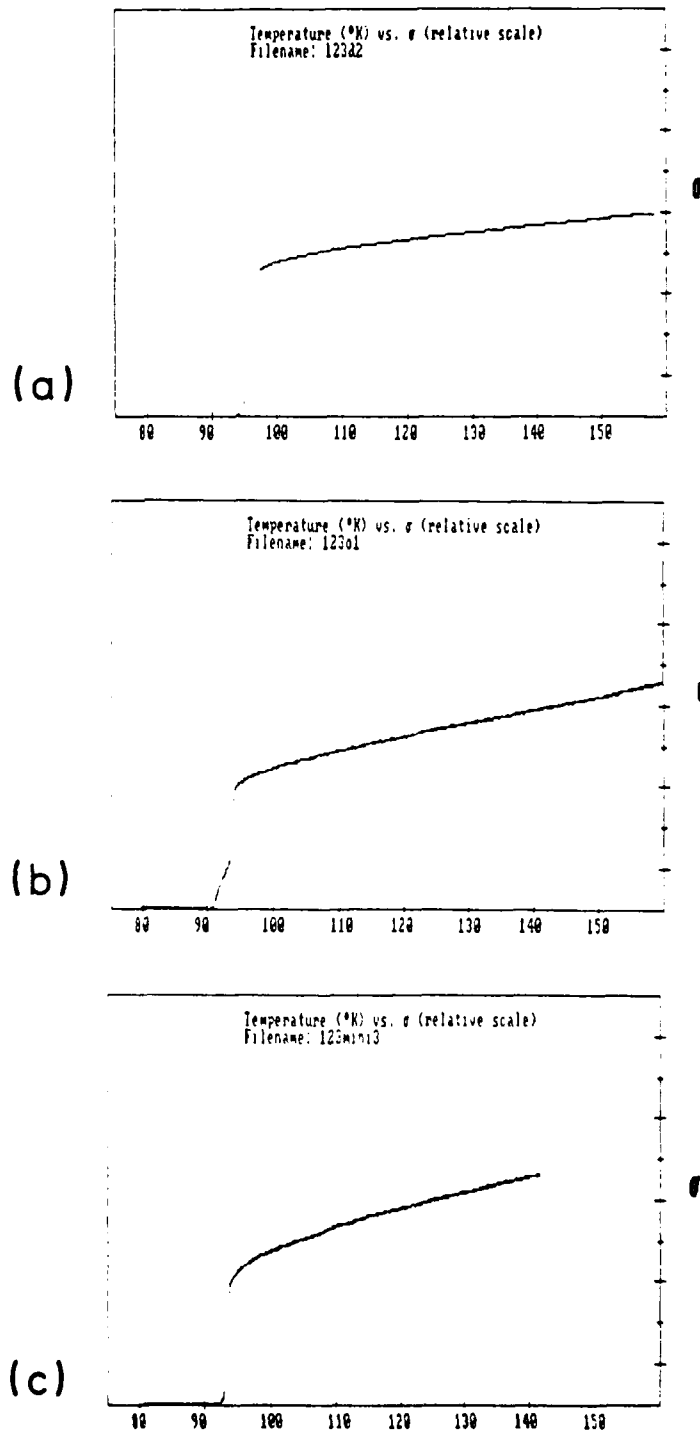


Figure 9 Results of D.C. resistivity measurements on (a) sample A, (b) sample B, and (c) sample C, respectively.

the conductivity of copper. The conductivity of copper changes as  $1/f^{1/2}$  and that of superconductor changes as  $1/f^2$ . Therefore, at lower frequencies in microwave range conductivity of these  $\text{YBa}_2\text{Cu}_3\text{O}_{7-x}$  samples will be significantly larger as compared to copper. In comparison to copper the superconductor samples do have at least metallic conductivity at room temperature and it increases with grain size and improved grain to grain interconnect.

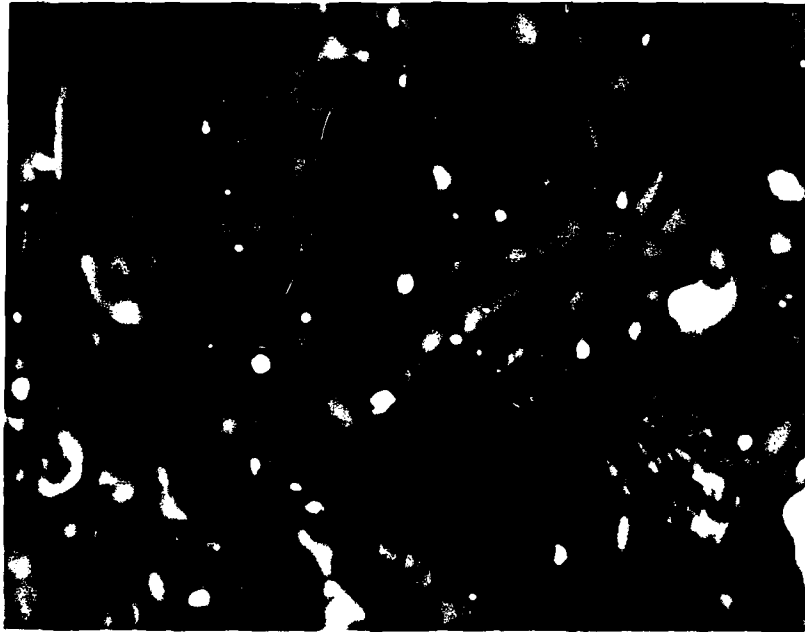
In the present measurements copper samples with the same dimension as superconductor samples were prepared. The shape of the samples were identical (i.e. cylindrical pallets) and the external dimensions were the same within 10%. However, the copper samples were in the form of solid slugs whereas superconductor samples were in the form of compacted and sintered discs with the packing density in the range of 60% to 80%. Hence, even in the best case sintered material does not have the surface as continuous as the casted material. Also, the grains in sintered material are not all oriented in a same crystallographic direction. It has been suggested [4] that in low temperature superconductors superconducting islands are connected by resistive paths. Similar resistive paths can be expected in high temperature superconductors if the microscopically observed intragranular "unfaceted" regions are not superconducting at 77°K. Meulenberg et al. [1] had suggested a material model for high  $T_c$  superconductors. According to this model bulk high  $T_c$  superconductor materials involve superconducting paths that are nonlinear and particularly just below the critical temperature may be circuitous. For DC measurements, such meandering paths have only a small effect which is seen during the onset of superconducting behavior. At this stage, intense magnetic fields from high local current densities can quench the superconductivity and force the current to flow, for short distances, through alternative paths, which may include resistive material. At high frequencies circuitous paths which result in self and mutual inductance can generate back-emfs that oppose current flow along the path and thus divert current through resistive channels. These inductive effects will increase with frequency. As temperatures are lowered below  $T_c$  and more superconducting paths are opened up, the current flows become more linear and the self inductance is reduced. Most applications require high conductivity and not zero resistance. Therefore, a means of reducing the inductive element of HTS materials, even at the expense of slightly increased resistive components, would be highly desirable. This could be accomplished by filling the voids in bulk HTS materials with high-conductivity materials. In the present case we used gold to fill these voids and test this model. At present we do not understand the nature of intragranular unfaceted material which is encountered the most in the material processed at 975°C. Hence, we decided to add gold in material processed at 960°C,

which has at least 50-60  $\mu\text{m}$  sized grain and has less of unfaceted material present in intergranular space. Using the same base material as in sample "B" we prepared HTS sample containing 10% gold by weight. The specimen weight and size were kept same as sample "B" and this sample was processed under identical conditions as the sample "B." We labeled this gold doped sample as "BG." Figure 10 is a microphotograph showing the grain structure of a sample "BG." The bright white spots in the photograph are gold particles. Comparing the microstructure of sample BG with that of Sample B (Figure 7(b)) it can be seen that the average grain size in gold doped sample is larger than that in the undoped sample. Authors have not come across a report in open literature, indicating the effect of gold doping to increase the grain size in these materials. Other effect of addition of a gold to this was found on the transition temperature. Figure 11 shows the results of D. C. resistivity measurements on gold doped sample. Addition of gold not only makes the superconducting transition sharp, but also increases the transition temperature by a few degrees. This can easily be seen by comparing Figure 9(b) with Figure 11. Superconducting grains in  $\text{YBa}_2\text{Cu}_3\text{O}_{7-x}$  can be identified by the presence of twins when observed under polarized light. A number of pure  $\text{YBa}_2\text{Cu}_3\text{O}_{7-x}$  and 10% gold doped  $\text{YBa}_2\text{Cu}_3\text{O}_{7-x}$  were observed under polarized light. In general most of the grains in gold doped samples showed the presence of twinned structure opposed to grains in undoped samples. Typical microstructure of gold doped and pure  $\text{YBa}_2\text{Cu}_3\text{O}_{7-x}$  samples observed using polarized light is shown in Figure 12(a) and 12(b).

The sample "BG" had a rough wedges around the periphery of the sample and reliable microwave measurements could not be carried out on this sample due to mounting problems. Hence, a new set of samples for the systematic study of the effect of gold were prepared.

About 50 gm of  $\text{YBa}_2\text{Cu}_3\text{O}_{7-x}$  was synthesized in pallet form at the processing temperature of  $960^\circ\text{C}$ . Out of this material three pallets each weighing about 2.5 gm and having diameters of 0.75 inch were made. The first pallet (sample X) was made of pure  $\text{YBa}_2\text{Cu}_3\text{O}_{7-x}$ . The second (sample Y) was doped with 10% gold (by weight), and the third pallet (sample Z) was doped with 20% gold.

The microstructure of these three superconducting pallets (i.e. X, Y, and Z) are shown in Figures 13(a), 13(b), and 13(c) respectively. The sample X consists of many faceted grains, most of which are columnar. The effect of addition of gold can be seen in the microstructure of sample Y. Sample Z, which contains 20% of gold by weight, also shows some grain growth, but is not as prominent as seen in sample Y. Sample Z also contains the large regions filled with



(X800)

Figure 10 Photograph showing the effect of the addition of gold on the microstructure of  $\text{YBa}_2\text{Cu}_3\text{O}_{7-x}$ . This sample was made using base material as in sample B and adding 10% gold by weight to it. It can be seen that compared to grain in sample B (Figure 7b) this sample has larger grains.

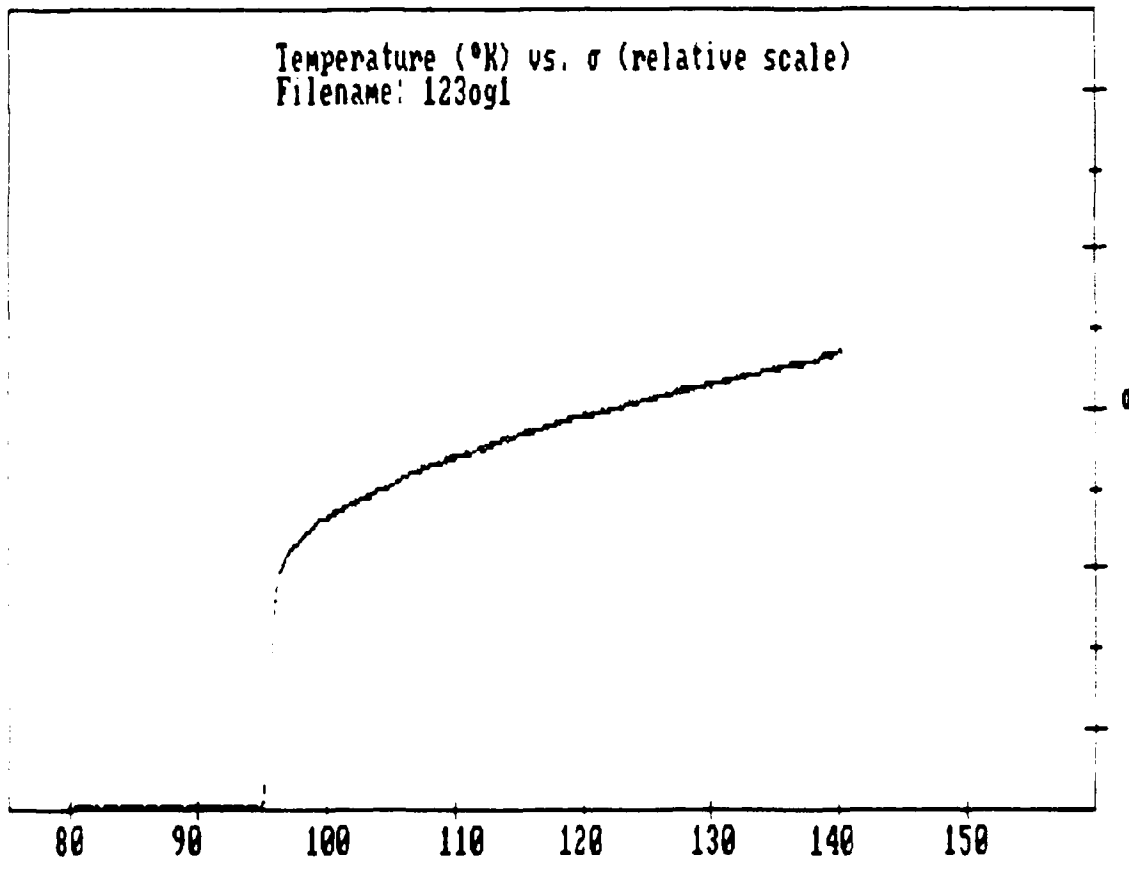


Figure 11 Results of D.C. resistivity measurements on gold doped  $\text{YBa}_2\text{Cu}_3\text{O}_{7-x}$  sample (sample BG).

(X500)



Figure 12 Microstructure of (a) pure and (b) gold doped  $\text{YBa}_2\text{Cu}_3\text{O}_{7-x}$  samples observed using polarized light. The grains with twinned regions indicate the presence of superconducting phase.



(a)



(b)



(c)

Figure 13 Photographs showing microstructures of pure and gold doped samples of  $\text{YBa}_2\text{Cu}_3\text{O}_{7-x}$ . (a) pure  $\text{YBa}_2\text{Cu}_3\text{O}_{7-x}$  (sample X), (b)  $\text{YBa}_2\text{Cu}_3\text{O}_{7-x}$  containing 10% gold by weight (sample Y), and (c)  $\text{YBa}_2\text{Cu}_3\text{O}_{7-x}$  containing 20% gold by weight (sample Z). (X400)

gold. These three samples were first characterized with respect to D.C. resistivity (Figures 14[a,b,c]). Then the microwave measurements were carried out on these samples (Table II). Finally, the A.C. susceptibility measurements were carried out on these samples (Figures 15[a,b,c]). The A.C. susceptibility measurements were carried out on pieces of about 5mm x 2mm x 2mm size. Both D.C. resistivity and A.C. susceptibility results suggest that superconducting properties can be enhanced by the addition of optimum amounts of gold. In order to determine this optimum amount, a further transient study with gold doping in the range of 0-20% gold is needed, which will be a subject of future study. Results of microwave measurements presented in Table II show that  $Q$  of the superconductor material containing 10% gold (sample Y) is almost equal to that of copper at 16 GHz. Understanding of exact mechanism by which gold in  $\text{YBa}_2\text{Cu}_3\text{O}_{7-x}$  increases the grain size and improves the D.C. as well as microwave conductivity needs the detailed investigation.

TABLE II

SAMPLE	TEMP	$C_f$ (GHz)	$\Delta_f$ (MHz)	$Q = C_f/\Delta_f$ (x1000)	$n$	$Q/Q_{Cu}$
copper	RT	15.707	1.1	14.28	6.3	--
copper	77°K	15.759	0.6	26.26	4.2	--
X	RT	15.312	2.5	6.12	4.2	.43
X	77°K	15.361	0.65	23.63	.75	.90
Y	RT	15.295	2.8	5.46	3.2	.38
Y	LN	15.342	0.60	25.57	0.66	.97
Z	RT	15.219	2.6	5.85	1	.41
Z	LN	15.335	0.7	21.91	.8	.83

The improvement in electrical conductivity may be explained, qualitatively, in terms of improved grain-to-grain contact. Also, gold will prevent the loss of oxygen from superconductor material at the sites where gold particles are localized. Grain growth similar to we have reported here was observed by Jeffrey and Archer [6] in case of sintered tungsten. The presence of thorium oxide, which is insoluble in tungsten, was found to have increased the grain growth in sintered tungsten when added in optimum concentration. When the amount of thorium oxide exceeds the optimum level, it impedes the formation of large grains.

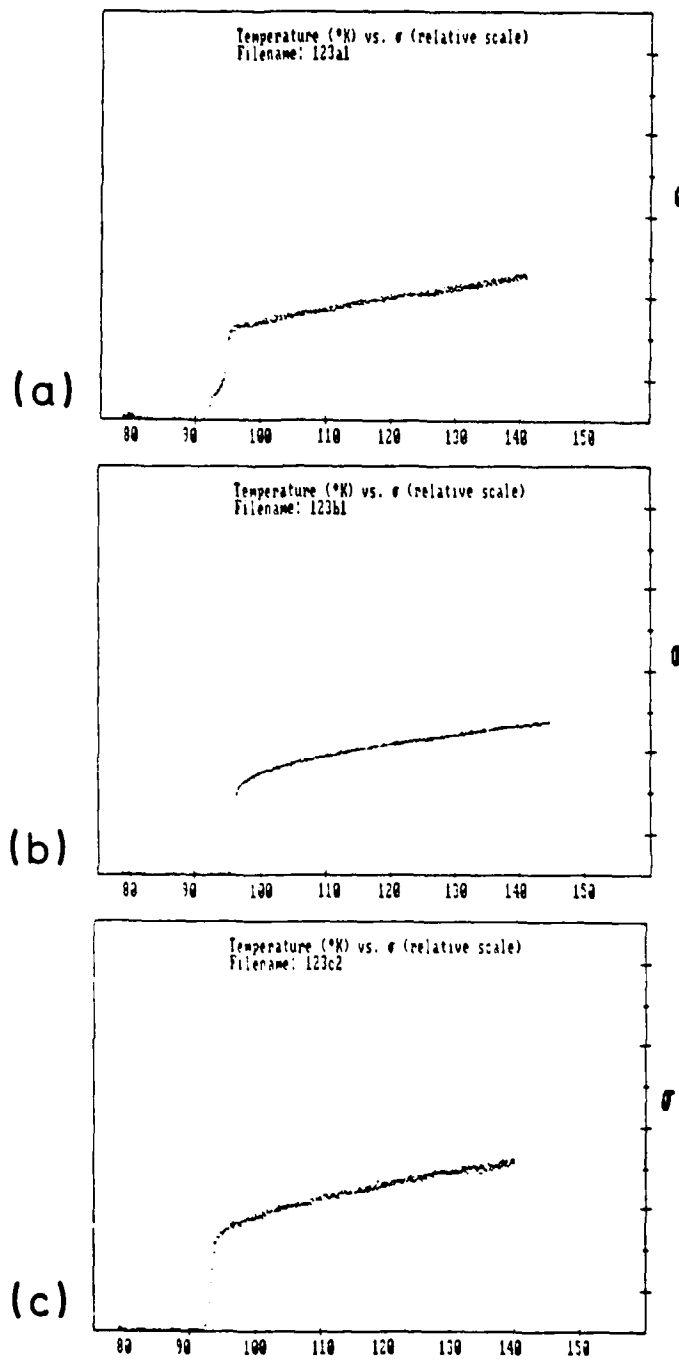
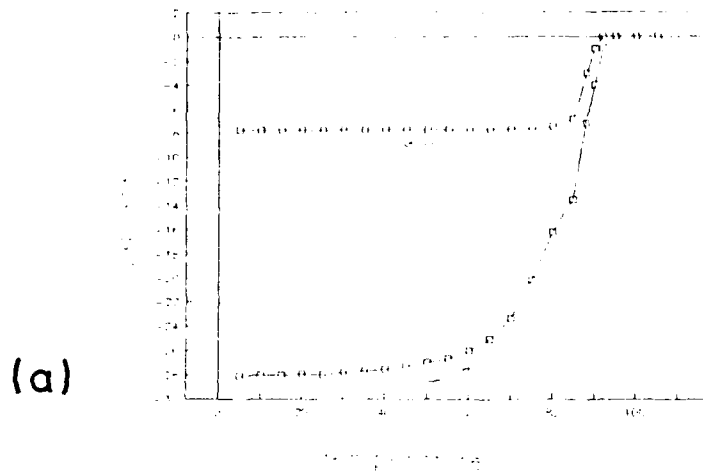
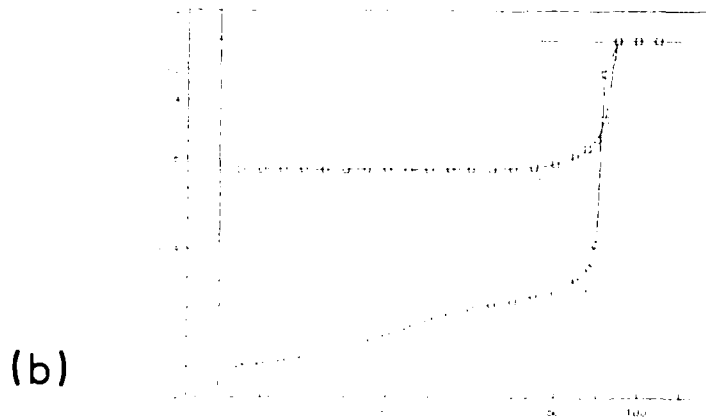


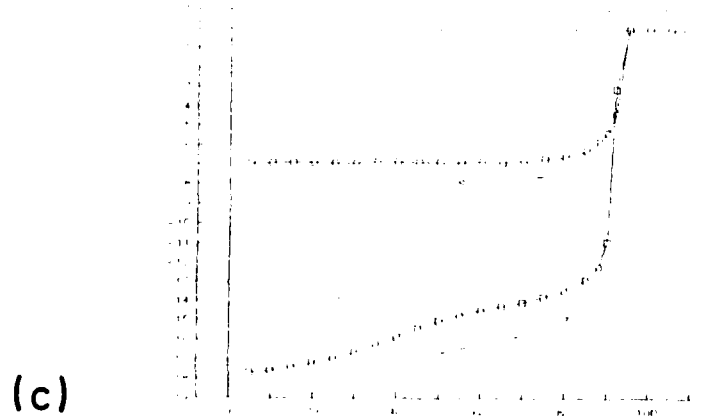
Figure 14 Results of D.C. resistivity measurements on (a) sample X, (b) sample Y, and (c) sample Z. It can be seen in (b) that with addition of 10% gold (by weight) to  $\text{YBa}_2\text{Cu}_3\text{O}_{7-x}$  the superconducting transition becomes sharp and the  $T_c$  and zero resistance temperature increases. As seen in (c) with increasing gold content, the superconducting properties deteriorates.



Graph (a) Sample X :  $\chi' = f(T)$



Graph (b) Sample Y :  $\chi' = f(T)$



Graph (c) Sample Z :  $\chi' = f(T)$

Figure 15 Results of A.C. susceptibility measurements on (a) sample X, (b) sample Y, and (c) sample Z. These results are in agreement with D.C. resistivity measurements shown in Figure 14a,b,c.

Using the material from the same batch which was used to make samples X, Y, and Z, two cylinders of length 0.5", inner diameter 0.5" and outer diameter 0.75", were fabricated. One cylinder was made of pure  $\text{YBa}_2\text{Cu}_3\text{O}_{7-x}$  and the second was doped with 10% (by weight) of gold. These cylinders were processed (oxygen annealed) at 960°C and found to have the same microstructure as pallets X and Y respectively. The x-ray diffraction pattern of these cylinders showed the presence of major peaks of  $\text{YBa}_2\text{Cu}_3\text{O}_{7-x}$ . These patterns are presented in Figure 16. These two cylinders will be delivered along with this technical report. Two more similar cylinders were made using the pure and 10% gold doped  $\text{YBa}_2\text{Cu}_3\text{O}_{7-x}$ . Attempts to measure the Q factor (at microwave frequencies) of cavities made using these cylinders are in progress. These measurements will also be carried out at COMSAT laboratories.

The present study does indicate the microwave properties of  $\text{YBa}_2\text{Cu}_3\text{O}_{7-x}$  can be improved by optimizing its microstructure. There are two more ways in which the grain size and grain-to-grain contact can be improved. The first method is lowering the  $\text{YBa}_2\text{Cu}_3\text{O}_{7-x}$  sample through a steep gradient. Initially, this method was used by R.C. DeVries [7] for the growth of large grains of barium titanate. Later, this technique has been applied to other materials by various workers.

The second method is a quench and melt growth process suggested by Masato Murakami [8]. The feasibility of this technique to obtain  $\text{YBa}_2\text{Cu}_3\text{O}_{7-x}$  of superior structure has been demonstrated by Japanese researchers. However, this process still requires optimization of several process parameters.

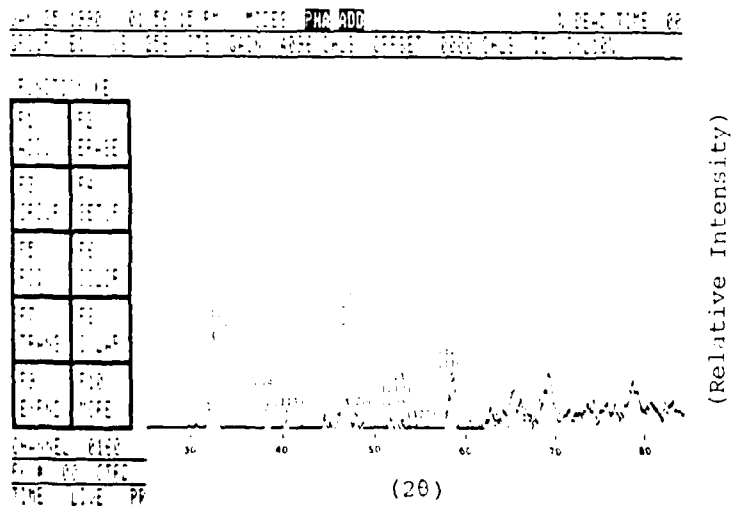


Figure 16 X-ray diffraction pattern of (a) pure and (b) gold doped  $\text{YBa}_2\text{Cu}_3\text{O}_{7-x}$  cylinders.

#### 4.0 CONCLUSION

1. The present study indicates that optimization of microstructure can improve the microwave conductivity of  $\text{YBa}_2\text{Cu}_3\text{O}_{7-x}$ . Optimum microstructure here refers to large grain size and better grain-to-grain contact.
2. In the present study we determined that  $\text{YBa}_2\text{Cu}_3\text{O}_{7-x}$  processed (oxygen annealed) at  $960^\circ\text{C}$  and  $975^\circ\text{C}$  yield grain size in the range of  $60\mu\text{m} - 150\mu\text{m}$ .
3. Addition of the optimum amount of gold to  $\text{YBa}_2\text{Cu}_3\text{O}_{7-x}$  results in a sharp superconducting transition and also increases the superconductor transition and zero resistivity temperatures.
4. Addition of gold also improves the microwave conductivity of  $\text{YBa}_2\text{Cu}_3\text{O}_{7-x}$ .
5.  $\text{YBa}_2\text{Cu}_3\text{O}_{7-x}$  processed at  $960^\circ\text{C}$  has conductivity equal to about 90% the conductivity of copper at 16 GHz. Addition of 10% of gold to this material increases its conductivity to about 97% the conductivity of copper at about 16 GHz. Addition of 20% of gold to this material deteriorates its microwave conductivity.
6. Interpolation of the results on microwave conductivity at 16 GHz to lower frequencies suggests that at lower frequencies our material has microwave conductivity higher than that of copper.

#### 5.0 ACKNOWLEDGMENTS

This research has been supported by SDIO under the SBIR program contract #F49620-89-C-0111. Dr. Harold Weinstock, Air Force Office of Scientific Research, Bolling Air Force Base, DC served as the technical monitor for this contract. Special thanks to Dr. Andrew Meulenberg of COMSAT Laboratories for his help in measurements of microwave conductivity of superconductor samples. His constant interest and stimulating discussions were very helpful. We would also, like to thank Dr. Richard Green, Director of Superconductor research at University of Maryland for his help in A.C. susceptibility measurements. The support of Kathy Aversa for the contract administration and preparation of this report is gratefully acknowledged. Our appreciation to Kristin Gianotti for her help during the preparation of the manuscript.

## 6.0 REFERENCES

1. A. Meulenberg, H-L. A. Hung, and G. H. Tough, "Microwave Characterization of Bulk and Powdered High  $T_c$  Superconductors," in Proceedings of International Conference on IR and MMW, (1988).
2. T. M. P. Percival, J. S. Thorn, and R. Driver, "Measurements of High  $T_c$  Superconductivity in a Microwave Cavity," Electron Lett., Vol. 23, no. 23, November 1987, p. 1225-1226.
3. D. S. Ginley, E. L. Venturini, J. F. Kwak, R. J. Baughman, and B. Morosin, "Improved Superconducting  $YBa_2Cu_3O_{6.9}$  Through High Temperature Processing," J. Material Research, May/June 1989, p. 496-500.
4. J. M. Tarascon, P. Barboux, B. G. Bagley, L. H. Greene, W. R. McKinnon, and G. W. Hull, "High Temperature Superconducting Oxide Synthesis and the Chemical Doping of Cu-O Planes," Chemistry of High Temperature Superconductors, Ed. David L. Nelso, M. Stanely Whittingham, and Thomas F. George, American Chemical Society, Washington, D.C., 1987, p. 198-210.
5. S. Sridhar, "Microwave Response of Thin-Film Superconductors," J. Appl. Phys., vol. 63, no. 1, January 1988, p. 159-166.
6. Z. Jeffrey and R. S. Archer, "The Science of Metals," McGraw-Hill, New York, (1924).
7. R.C. DeVries unpublished work described in "The Art and Science of Growing Crystals," edited by J. J. Gilman, John Wiley and Sons, p. 473, (1968).
8. The quench and melt growth process is described by Masato Murakami in "Supercurrents," vol. 9, July 1989, p. 41-47.

## Appendix A

Description of CPSD and its calibration.

In x-ray diffractometry experiments, observations with a good spatial resolution over a wide range are required. CPS 120 can be mounted on all kinds of goniometers now available on the market and its electronic data can be processed by all data processing systems. CPS 120 is a sophisticated tool which uses the latest developments in detector technology. CPS 120 can replace films and proportional scintillation detectors as well as scanning straight position sensitive detectors with great advantages for all x-ray diffraction applications.

### THE SYSTEM

The CPS 120 system includes:

- The detector with its preamplifier
- The electronic system

The Detector:

The detector is a gas flow blade chamber. It thus has a curved anode accurately located on the circle of the goniometer. The x-ray peak position is obtained through the so-called delay line readout method.

A good spatial resolution - less than  $0.02^\circ$  - is secured with the use of special materials very accurately manufactured. The anode made with a blade can receive the direct x-rays beam.

The anode signal can be used to control the exact count rate of x-rays radiating over the detector. The pulses from both sides of the delay-line serve to calculate the x-ray position impact.

The preamplifier is used to adapt the electronic pulses collected on the delay-line to the electronic system.

The Electronic System:

The electronics is made up of specific NIM modules. Each module has a determined and independent function - the electronic system includes: a PC module (pressure and gas flow control); a HV module (high voltage power supply); a ratemeter module - this is helpful for the tuning of the goniometer and enables to control the count rate of x-rays radiating over the detector.

A APD module - these discriminators accurately define the centroid of pulses coming from the detector and so they help determine the exact position of x-rays. A DDL module is used to add or subtract some delay. This module is useful when the users of CPS 120 want to zoom any part of the x-ray diffraction pattern. A PSP module - it gives the position of x-rays, and its output can be connected to all (analog to digital convertors) available in the market.

CPSD chamber consists mainly of Anode and Cathode, and a stream of ionizing gas (Argon + 15% Ethane) flowing at a constant pressure of 6.5 Bars. A schematic illustrating CPSD construction is shown in Figure 1. When a direct or diffracted beam enters the detector chamber, it ionizes the gas and produces electron-positive ion (cation) pairs.

Due to high voltage between anode and cathode, electrons are attracted to the anode and travel with very high velocity. This produces an electron avalanche. Because the electron avalanche is sharply localized, the point where electrons hit the anode can be electronically determined by measuring the time required for the pulse to travel from the point of impact to the end of the anode. This provides the angular position ( $2\theta$ ) of the x-ray beam. A circuit diagram illustrating operation of CPSD is given in Figure 2. The CPSD used in this work has the angular range of  $120^\circ$ , hence diffraction peaks in this wide range can be simultaneously obtained without moving the detector, unlike the conventional diffractometry.

Before operating the CPSD unit, high purity gas mixture containing Argon and 15% Ethane was allowed to flow at a recommended pressure (6.5 Bars) through the detector chamber for about 24 hours. Using the direct x-ray beam, operation of the CPSD and associated electronics and software has been tested. The height of CPSD was adjusted such that the direct beam is incident in the middle of the chamber. The zero of the detector was adjusted as described in the operation manual. Next, the direct beam was recorded for 60 seconds at various detector positions from one end to the other end. This calibrated channels in terms of angle  $2\theta$  (in degrees). This will help identify peak position for the main as well as diffracted x-ray beams. Table I and corresponding Figure 3 respectively represent the calibration run. Next, this calibration was verified using x-ray diffraction of aluminum. Diffraction pattern for this sample was recorded in  $120^\circ$  range. The diffraction peaks were identified and matched with JCPDS diffraction file on aluminum. These results are presented in Table II and Figure 4 respectively. Accuracy better than 1% was observed for angles less than  $120^\circ$ . Present CPSD can record  $2\theta$  angles up to about  $150^\circ$ . For angles greater than  $120^\circ$ , the accuracy goes down to 15%. It is recommended for the use in the  $120^\circ$  range with angular resolution of  $0.018^\circ$ .

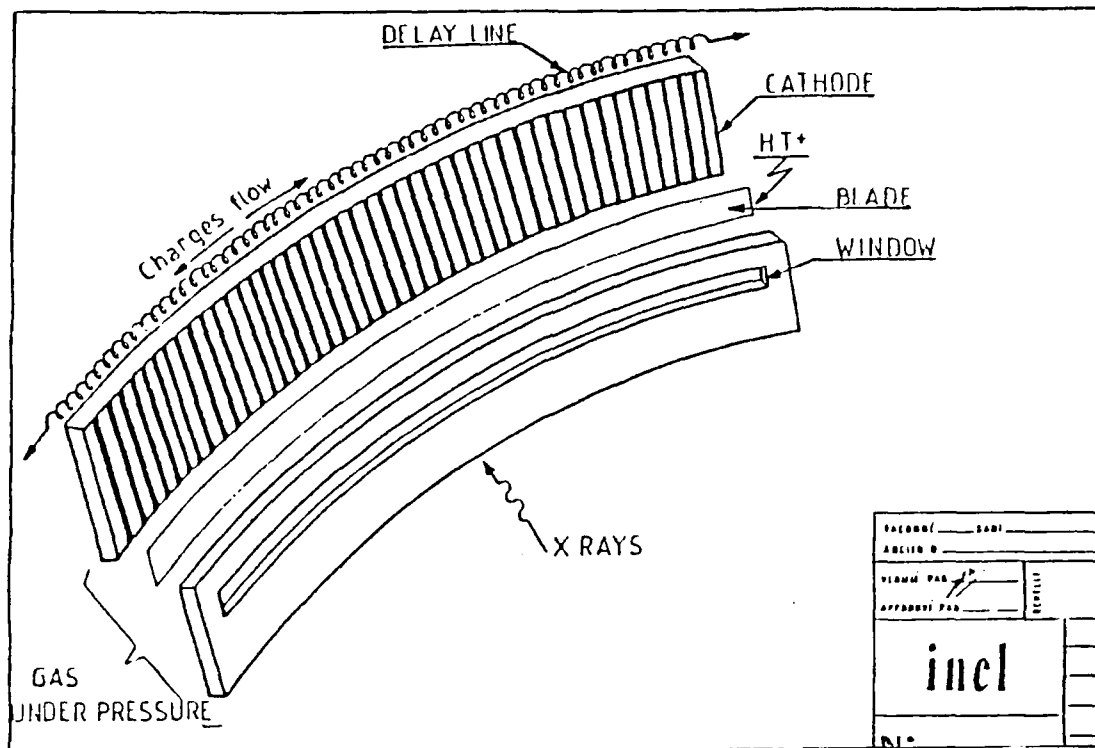


Figure 1 Schematic Illustrating the Construction of CPSD.

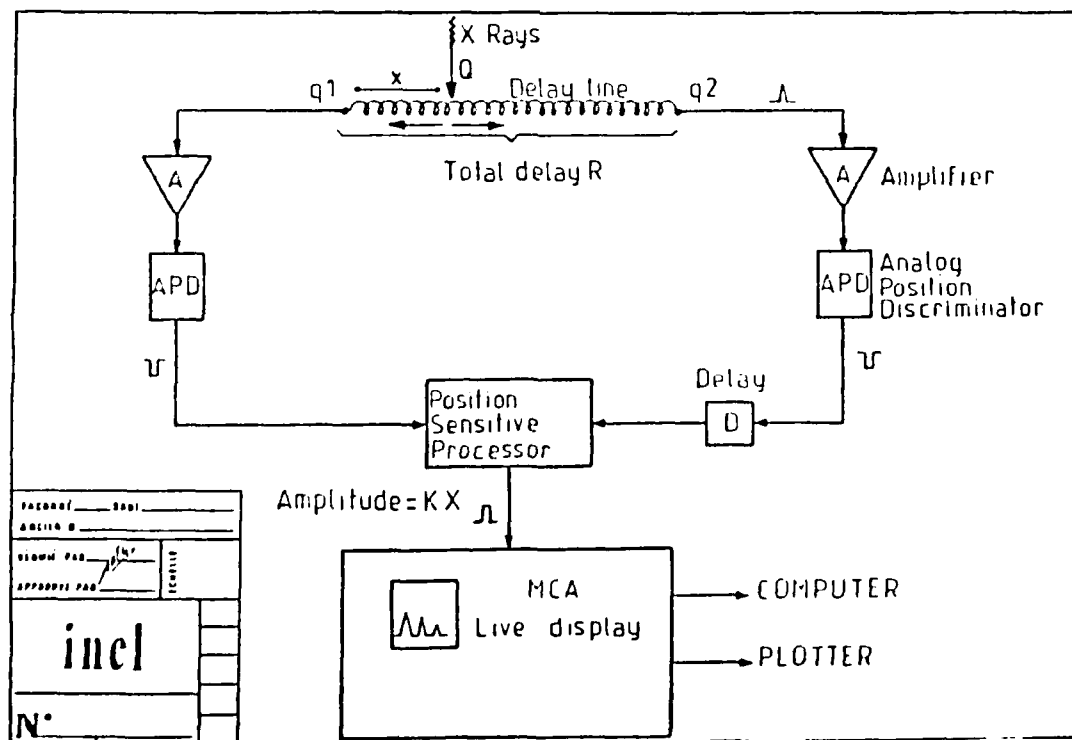


Figure 2 Electrical Circuit Illustrating the Operation of CPSD.

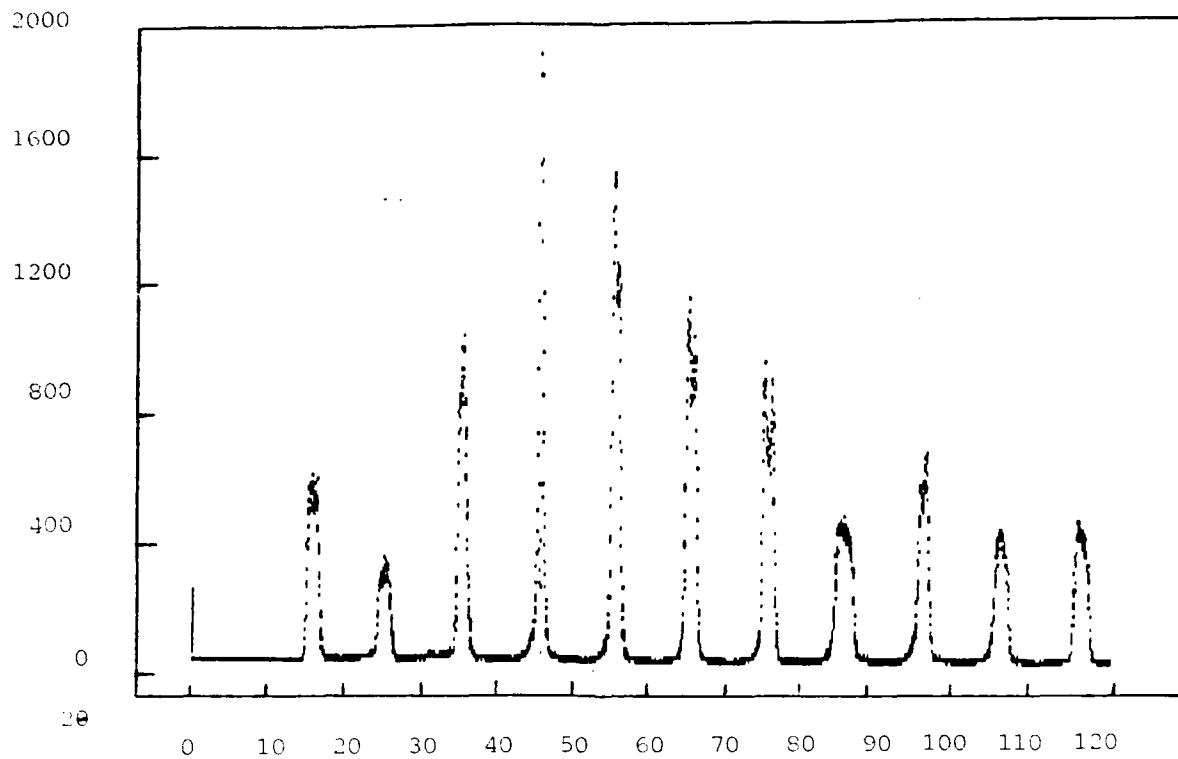


Figure 3 Calibration Run (using Main Beam).

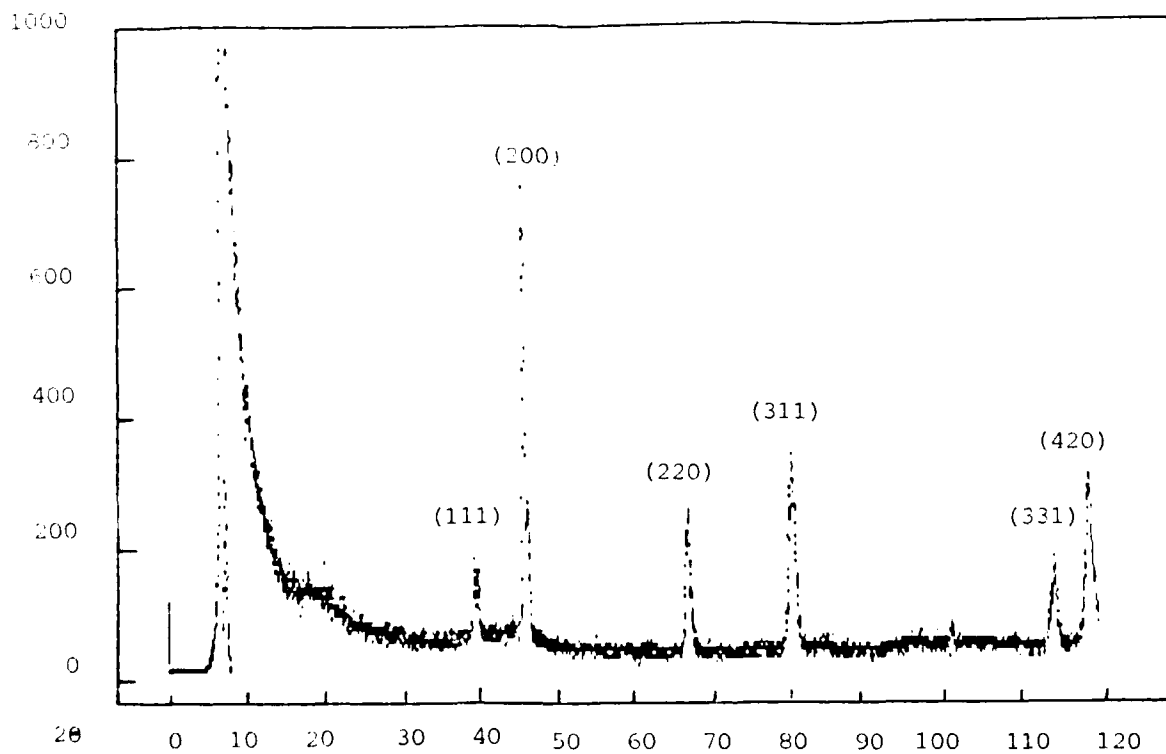


Figure 4 Aluminum Diffraction Pattern Obtained using CPSD.

TABLE I

2	Channel #	Number of Channels per 10 <sup>0</sup> (Δ C/10 <sup>0</sup> )
134	529	324
125	853	349
115	1202	340
105	1542	331
95	1873	336
85	2209	344
75	2553	343
65	2896	385
55	3281	325
45	3606	353
35	3959	346
25	4305	346
15	4316	

$C/10^{\circ}C = 343.3 = \text{Average Number of Channels per } 10^{\circ} \text{ Span}$

$C/1^{\circ}C = 34.3 = \text{Number of Channels per Degree}$

TABLE II

(hkl)	$d$ Å	$2\theta$ (in degrees)
(111)	2.3373	38.4690
(200)	2.0225	44.7556
(220)	1.4157	65.8958
(311)	1.2061	79.3462
(331)	0.9222	113.2058
(420)	0.8995	117.7380

Aluminum Powder Diffraction Data Obtained using CPSD.